FDR4ALT

Validation Report Document : Ocean Waves TDP

CLS-ENV-NT-23-0419

Issue 4.1 – 03/07/2023

Public

AUTHORS TABLE

Object	Name
Authors	Annabelle Ollivier, Victor Quet, Fanny Piras (CLS)
Checked by	Gabriele Brizzi (SERCO) and Pierre Féménias (ESA)
Accepted by	Pierre Féménias (ESA)

CHRONOLOGY ISSUES

Issue	Date	Object
1.0	17/05/22	Draft version for Phase 2 PM#1
2.0	02/12/22	Intermediate version for Phase 2 PM #1 (80% completed for ENVISAT)
3.0	02/05/23	Final version for Final Review
4.0	23/05/23	Final version for Final Review with RIDs implemented
4.1	03/07/2023	Final version: document divided into distinct reports

TABLE OF CONTENT

LIST OF FIGURES

LIST OF TABLES

1 Introduction

This document has been written in the frame of the FDR4ALT project, ESA contract N°4000128220/19/I-BG. It is a deliverable of task 4 of the project and is identified as [D-4-02].

1.1 The FDR4ALT Project

In the framework of the European Long Term Data Preservation Program (LTDP+) which aims at generating innovative Earth system data records named Fundamental Data Records (basically level 1 altimeter and radiometer data) and Thematic Data Records (basically level 2+ geophysical products), ESA/ESRIN has launched a reprocessing activity of ERS-1, ERS-2 and ENVISAT altimeter and radiometer dataset, called the FDR4ALT project (Fundamental Data Records for Altimetry). A large consortium of thematic experts has been formed to perform these activities which are:

1) To define products including the long, harmonized record of uncertainty-quantified observations.

2) To define the most appropriate level 1 and level 2 processing.

3) To reprocess the whole times series according to the predefined processing.

4) To validate the different products and provide them to large communities of users focused on the observation of the atmosphere, ocean topography, ocean waves, coastal, hydrology, sea ice, ice sheet regions.

1.2 Purpose and scope of the validation report

After the FDR/TDP definition step and all benchmarking (Round Robin) between standard solutions addressed by each expert group, comes the production and validation step.

The objective of this document is to provide a validation report for the Ocean Waves TDP, following the strategy defined in the Validation Plan Document [D-4-01]. Note that to avoid heavy documents, the validation reports have been divided: there is one validation report for the FDRs (ALT FDR and MWR FDR) and one validation for each of the six TDPs. This document therefore contains only results for the **Ocean Waves TDP**.

This document describes in detail the validation that has been performed for the Ocean Waves TDP to assess the performances of the FDR4ALT final products. The validation covers the full lifespan of the missions and therefore includes long-term analysis, as well as cyclic analysis or targeted analysis that are relevant for this TDP.

2 Terminology

This section aims at defining clearly the terminology used in the FDR4ALT deliverables.

- **Product** refers a specific type of file, defined and described by a dedicated handbook, and designed for a clear purpose (the FDR4ALT project, the REAPER project, …). It is a “container”. One product refers to one file. The use of plural is designed to refer to a group of files, for instance the Thematic Data Products. “FDR4ALT products” will usually refer to all TDPs and FDRs, i.e., the outputs of the whole project. Note that the word "product" does not imply any notion of start date or end date, whereas "dataset" does.

- **File** can be used to refer to one single product or any other file that is not a product.
- **Parameter or variable** refers to a product's field, i.e., the content of the product. For instance, the sea level anomaly is a parameter of the Ocean & Coastal Thematic Data Products.
  Dataset can be used to refer to any group of data, not necessarily products. However, in the context of this project, it will often be used to refer to a sub-ensemble of products, on a specific period of time or a specific geographic area. For instance, the TDS (test dataset) refers to a dataset of 3 years of test products.

3 Ocean Waves Thematic Data Products

3.1 Introduction

This section addresses the validation of the Ocean Waves Thematic Data Products. It includes the coverage of valid data, the validation of the SWH data itself and the uncertainty field associated to the data. One part of the work is performed over one cycle, and the other one is performed over the whole period, from a climate application point of view. For the latter, metrics regarding the validation of the calibration step between ERS and ENVISAT are also given.

3.1.1 Validation datasets

To validate the delivered data in an efficient way, several datasets were compared to evidence finer structures in our data.

Those datasets are the following:

The FDR4ALT solution:

- ✓ FDR4ALT Adaptive retracking outputs compressed at 5 Hz from this dedicated TDP, with and without EMD filtering.

The references:

- ✓ FDR4ALT Adaptive retracking outputs at 20 Hz computed in the frame of this project (Detailed Processing Model Document section 4.1).
- ✓ CCI Sea State v2 products at 1 Hz: Second version of the reference dataset provided by the CCI for several altimetric missions.
- ✓ Official ENVISAT L2 products at 20 Hz from V3.0 reprocessing obtained with the MLE3 retracking: previous version of ENVISAT data.
- ✓ ERA5 (model) SWH dataset.

3.2 Validation Results

This section presents the different results obtained with the FDR4ALT dataset when compared with the previous version of ENVISAT products and the CCI Sea State dataset.

It is divided in three steps which are the following:

- ✓ The validation of the data selection step
- ✓ The validation over a first period of two years
- ✓ Finer results performed on one cycle of data.

✓ Global results validating the dataset on the whole time period

3.2.1 Selection/mapping step

A dedicated flagging was tuned for the Ocean Waves TDP, to extract as much relevant information as possible, at the chosen rate. The selection relaxed compared to the Ocean and Coastal TDP, essentially depends on the retracker's capacity to retrieve metrics but is not dependent to the availability of height dependent corrections.

In order to allow more natural variability for higher SWH, the threshold on the SWH noise is linearly SWH dependent.

Figure 3-1 shows the dispersion diagram of the standard deviation of the residual (SWH -SWH-ERA5) plotted per bin of SWH (10cm step). A linear fit between 2m and 6 m is then computed, and the flagging is tuned so that at 2m, data above 3 sigma is removed. This process has been computed for both ENVISAT and ERS data and presented in the following figure.

Figure 3-1 shows that the high frequency content of waves, (speckle noise, correlation effects and signal not captured by ERA5 model) is reduced with FDR4ALT data compared with the previous version of ENVISAT.

This is mainly dominated by the noise reduction as shown in the validation of Adaptive method.

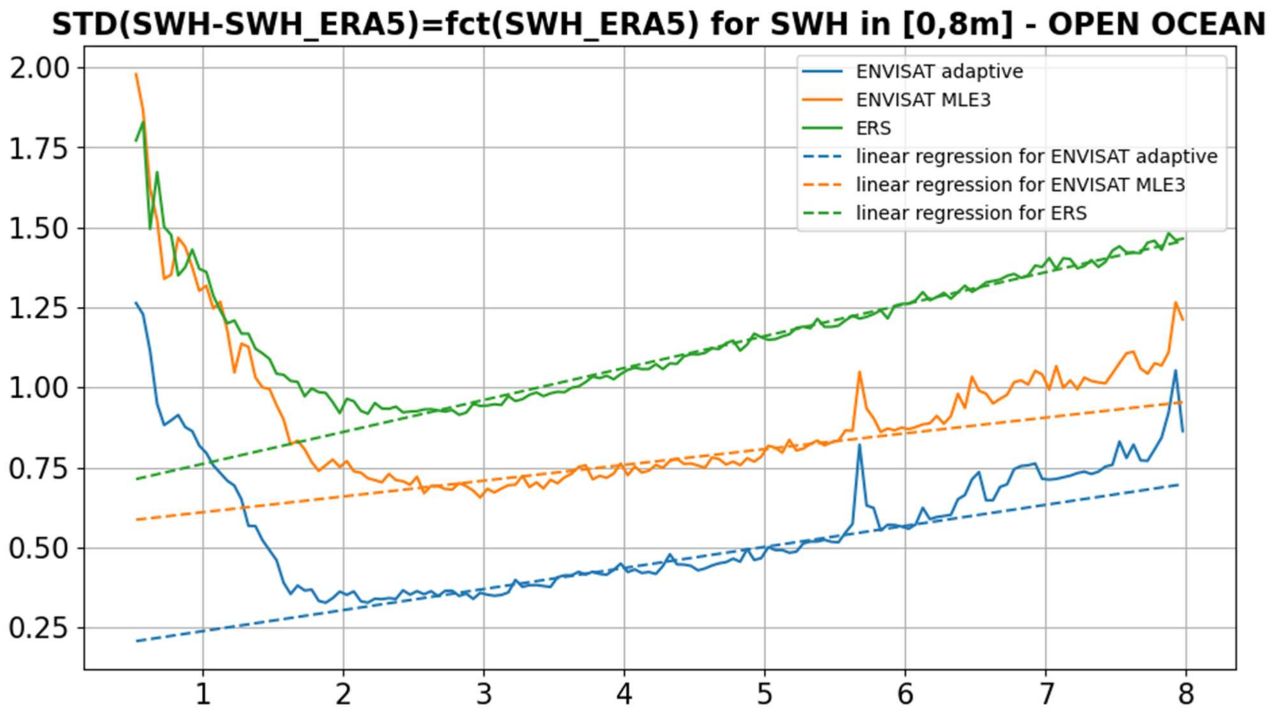

Figure 3-1 – Computation of the slope of the linear regression of the standard deviation of the residual between SWH values from ERS/ENVISAT and ERA5 model.

Linear coefficients are as follows:

- 0.07 m/m for ENVISAT adaptive data
- 0.1 m/m for ERS data

The increase of the high frequency content of nadir waves data is more important in ERS than in ENVISAT data. It is consistent with the important differences of noise level between ENVISAT adaptive data and ERS data that is illustrated in Figure 3-4 which presents a spectral analysis of all missions.

3.2.2 Validation over the first period

This section aims at presenting the results obtained with the data selection algorithm over a two years period for each mission. A time series of the percentage of invalid data per day and a map of percentage of invalid data per geographical boxes were computed.

ENVISAT

Figure 3-2 and Figure 3-3 illustrate the behaviour of the validation flag.

The stability of data selection is illustrated by Figure 4-6. The percentage is given with respect to global data (including land and sea-ice data).

All data on land are well removed and so are data in sea ice area are. In sea-ice area, a natural oscillation of presence of seasonal ice coverage in each hemisphere.

Finally, as the selection step was tuned depending on SWH values, a lot of high SWH values are kept in high latitudes.

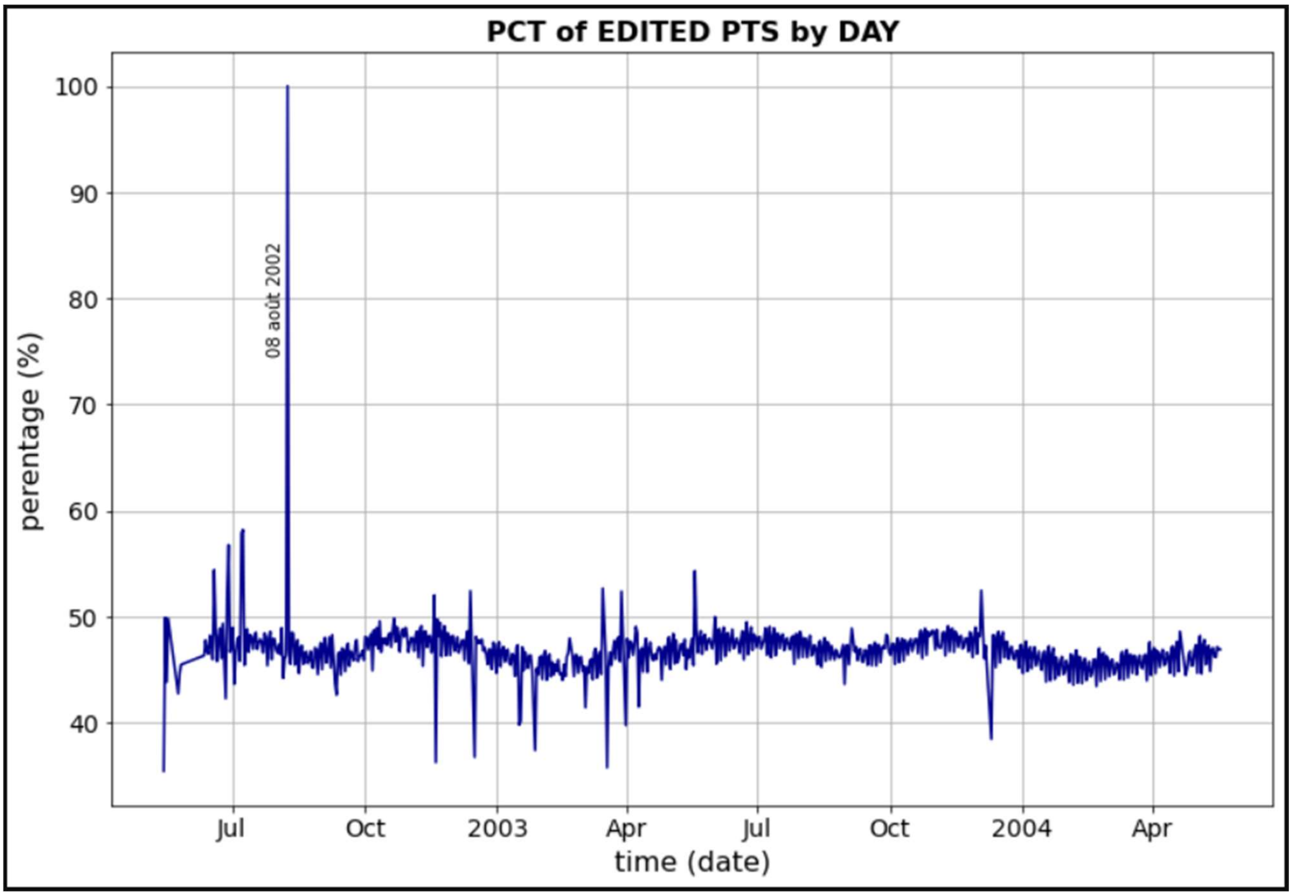

Figure 3-2 – Percentage of edited and Default Value points per day from cycle 6 to 26 in ENVISAT data

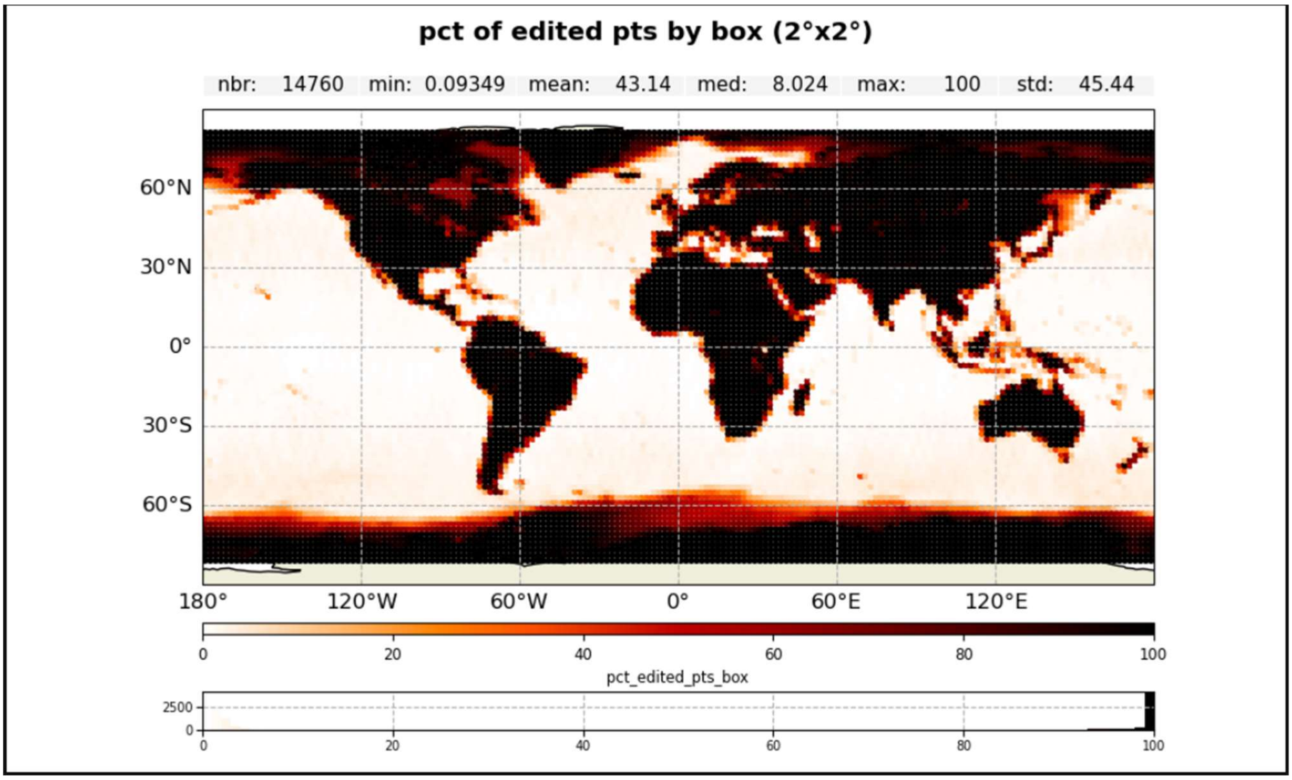

Figure 3-3 – Percentage of edited and Default Value points per geographical boxes (2° x 2°) from cycle 6 to 26 in ENVISAT data

Except near coast and ice, no particular pattern is identified when averaged over the whole period. Highlighting a very good availability of data over ocean.

3.2.3 Validation over one cycle

This section presents some diagnoses performed to evaluate the quality of FDR4ALT data when compared with the previous version of ENVISAT products and the CCI Sea State dataset.

First, a spectral analysis has been carried out on all datasets. Then, three diagnoses to illustrate the better approach to the coast of the FDR4ALT dataset. The last sub section is dedicated to uncertainties values delivered with wave heights data.

ENVISAT (cycle 25)

Spectral Analysis:

The spectral analysis in Figure 3-4 shows a great improvement of the Adaptive retracking when compared to the MLE3 retracking (previous version of ENVISAT products from the previous reprocessing). The white noise plateau has a lower level.

The performance of the resampling is as expected as the signal is cut right after the bump.

The High Frequency Adjustment (HFA algorithm) allows to decrease the white noise level, and the EMD filtering (Empirical Mode Decomposition) removes the spectral bump around 10 km.

CCI spectrum at 1Hz, seems affected by a correlated noise below 100km, removed on the denoised spectrum which decreases linearly until around 30km.

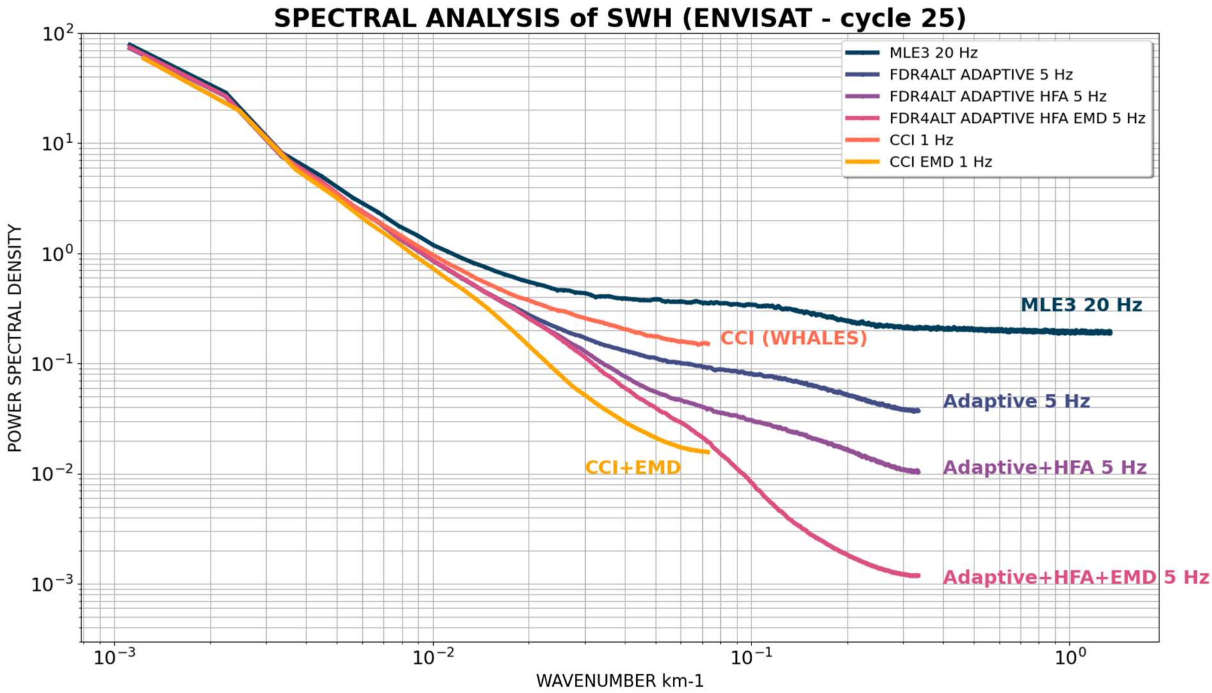

Figure 3-4 – Spectral analysis of ENVISAT data in different datasets over cycle 25

Better approach to the coast:

Thanks to our post processing, the FDR4ALT Ocean Waves TDP will enable to get closer to the shore with a higher precision and a better coverage than the current CCI Sea State filtered dataset. Below 40km, the coverage is up to 30% better and quite equivalent to the 20Hz dataset except for the very last 5 km, impacted by the altimeter footprint. The difference with the model also changes from the CCI dataset with relevant structures below 10km as shown in the rest of the section, notably on lagoon areas protected by coral reefs (see Figure *3-6*). The importance of near shore areas for climate subduction studies could make this new dataset very useful for the community.

However, the MLE3 retracking, with the same algorithm for the computation of the validation flag (changing the specific parameters such as the slope that depends on the behaviour of the data), a few points are lost in the first km from the coast. However, the improvement of the quality of data obtained with the Adaptive retracking is worth the loss of those few points (see Figure 3-5 and Figure 3-6).

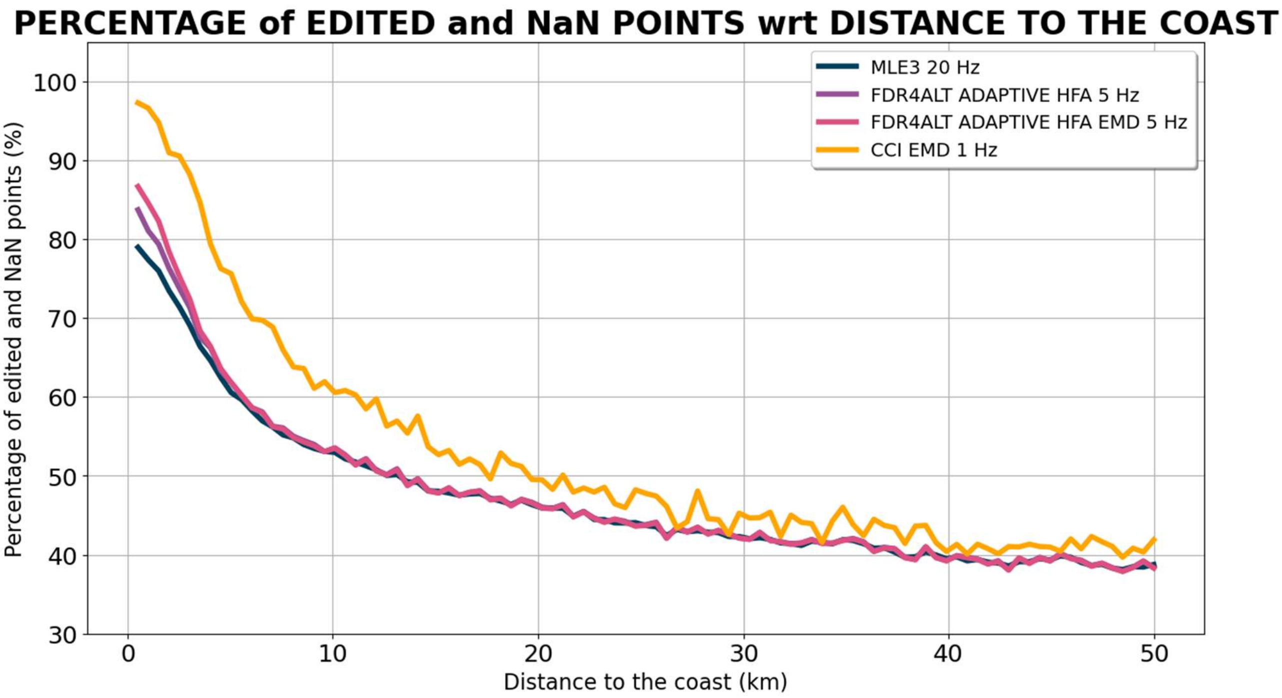

Figure 3-5 – Percentage of edited and Default Value points with respect to the distance to the coast in ENVISAT data

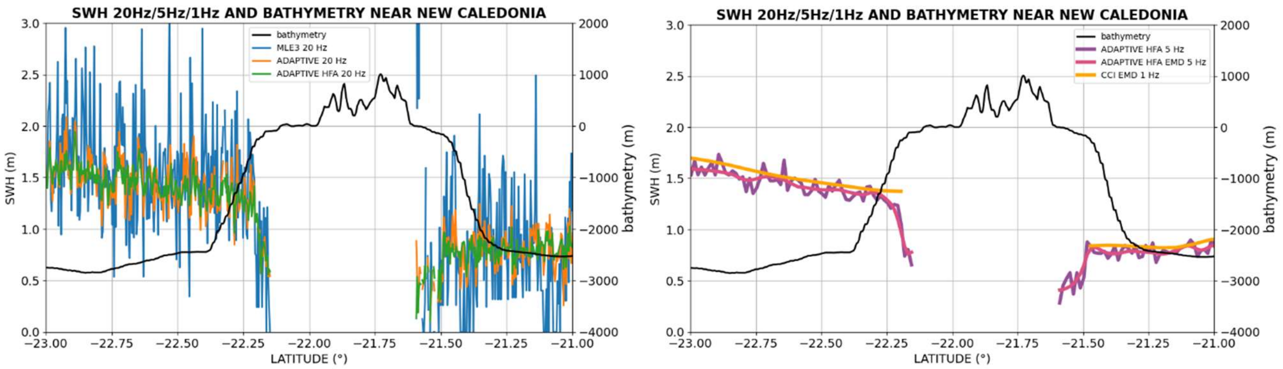

Figure 3-6 – Along track plot of ENVISAT data from cycle 25 / pass 288 near New Caledonia at 20 Hz (left) and 5 Hz / 1 Hz (right)

Finally, Figure 3-6 is a clear illustration of the improvement brought by this new version of ENVISAT products: The bias with the ERA5 model is reduced by far when compared with products from the previous reprocessing of ENVISAT data and with the CCI Sea State Dataset.

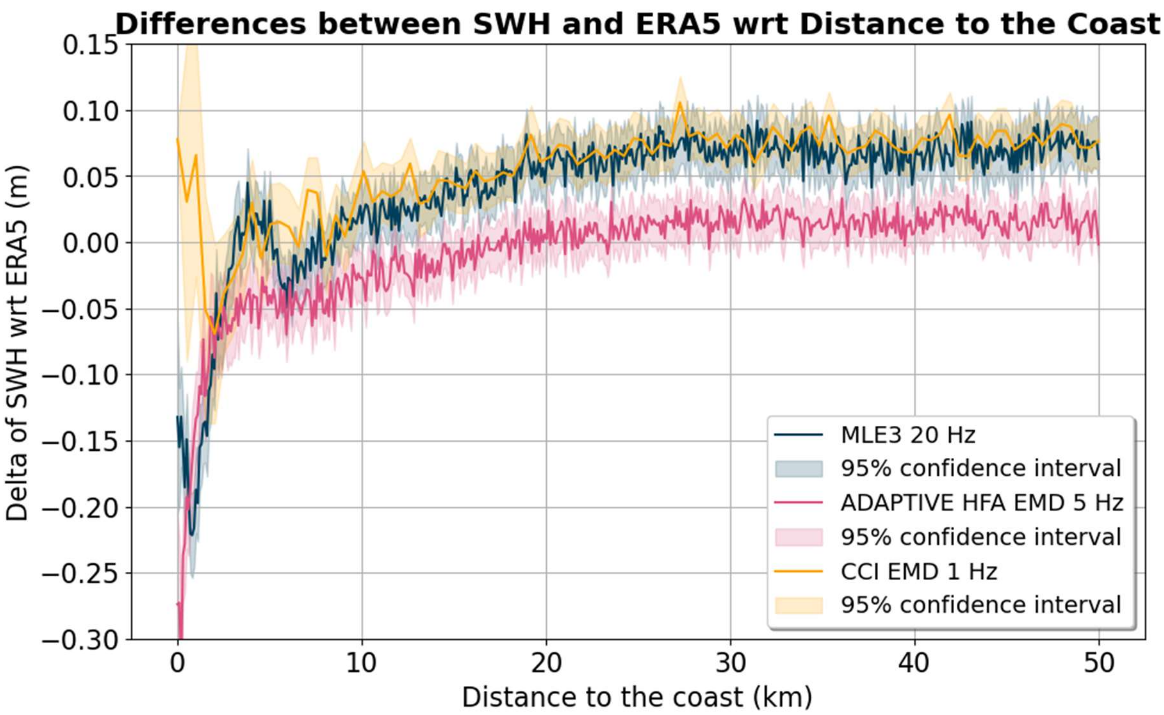

Figure 3-7 – Binned statistics of differences between SWH measured by ENVISAT and SWH from the ERA5 model with respect to the distance to the coast.

Added value signal around 10 km:

The aim of computing a 5Hz dataset is to study the higher variability and to remove the decorrelated noise above 2km. Thanks to this, along track plots (Figure 3-8) enable to see finer structures and a kind of oscillation at around 10km that we focused on. We make the hypothesis that they exist on the zones where the spectra have a stronger bump than elsewhere and for this, we compute spectra in geographical 10°x10° boxes and we estimate the energy of 20Hz spectra between 7.5 and 12.5 km (left) et 2 et 2.5km (right). The result is plotted on Figure 3-9. The plateau height (right) does not depend on the localization of the spectrum whereas the bump energy (left) has a clear geographical pattern totally correlated with the period of the waves as seen also for Jason3 mission on Figure 3-10.

These effects need further analysis but could be the signature of wave group modes, never observed until then with altimetry. Such phenomena, related to constructive/destructive interferences can reach around 10% of SWH at these scales (10km) (See [**RD 17**

The FDR4ALT Adaptive SWH 5Hz products will enable such studies on ENVISAT, among other missions.

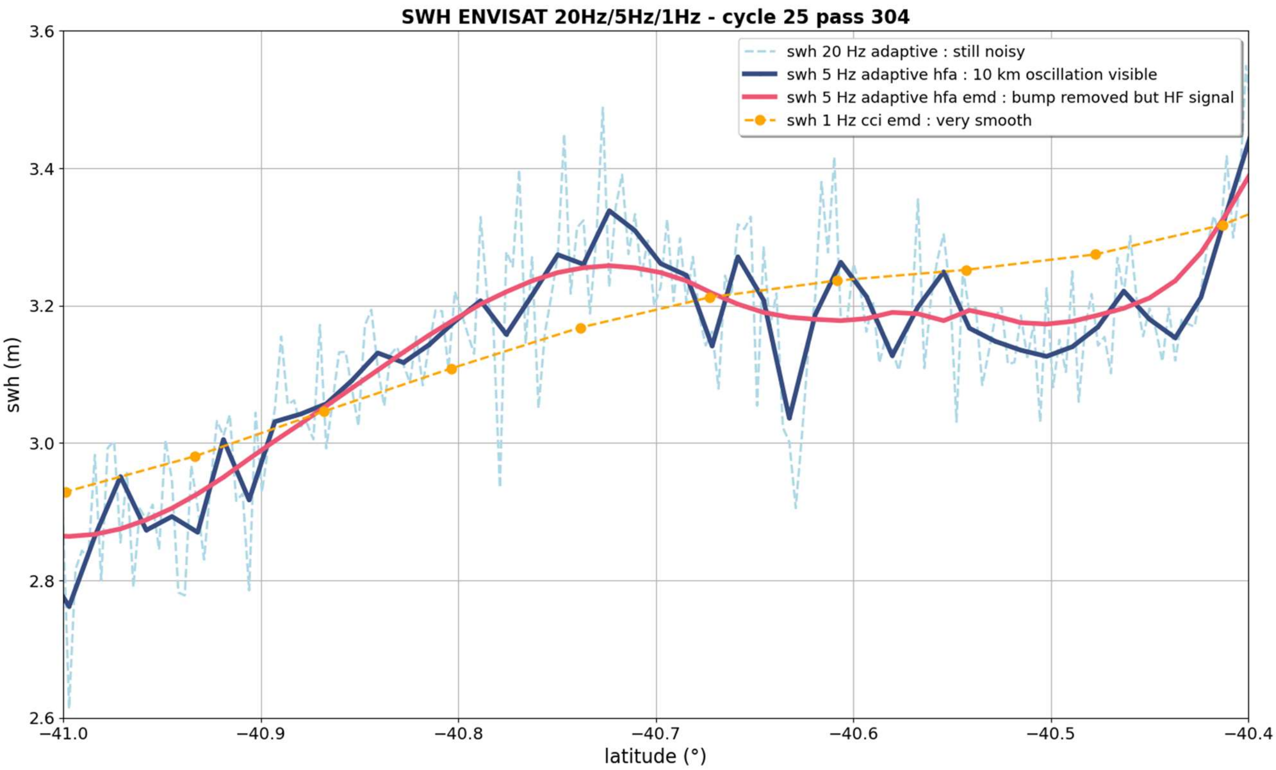

Figure 3-8 : Ocean Waves TDP. Along track profiles of 20Hz Adaptive SWH (pink), 5Hz Adaptive SWH (green) 1Hz CCI Sea State denoised (dark blue) SWH

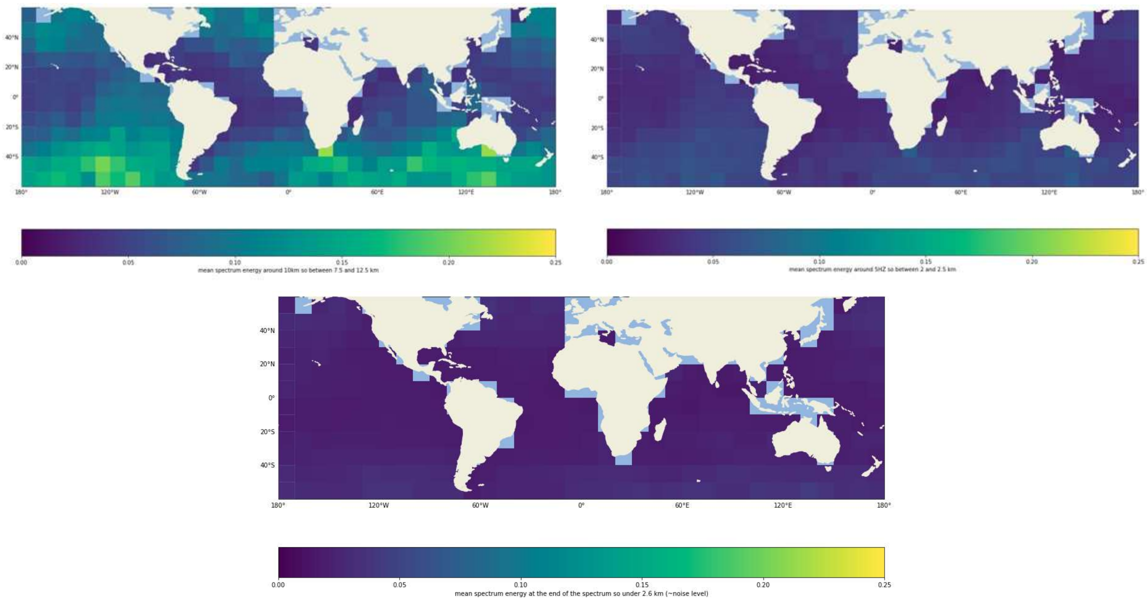

Figure 3-9 : Ocean Waves TDP. For 10°x10° boxes, mean spectrum energy computed around the 10km bump (top left), at the end of the 5Hz spectrum (top right) and on the noise plateau (bottom) (over cycle 25) for Adaptive SWH data.

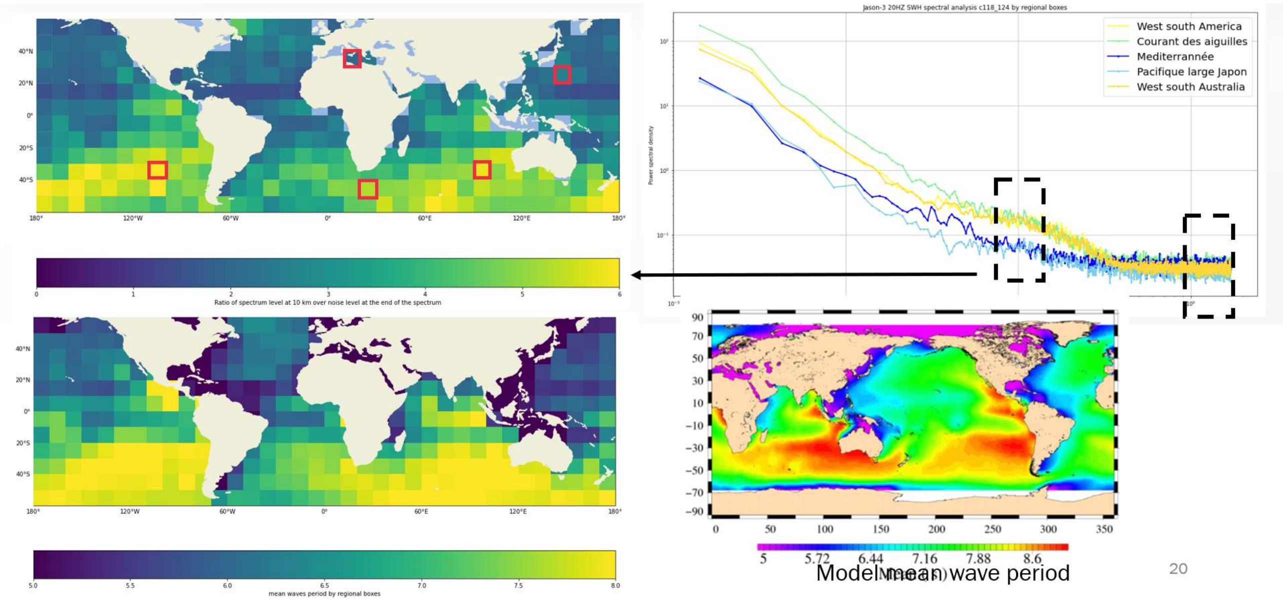

Figure 3-10 : Ocean Waves TDP. For J3 mission A (top left) Ratio of mean spectrum energy computed around the 10km bump as shown on B for 5 specific boxes (top right). C (bottom left) collocated average Period from WAM model over the same period (2 months from cycles 108 to 127).

See more details in.

Uncertainties:

Figure 3-11 represents the values of the swh uncertainty field. Some geographical structures appear from this diagnosis. The uncertainty is higher in areas where the sea state is mostly composed by well-structured swells with high wavelengths/wave period. Those are the area responsible of the spectral bump at 10 km. This figure is to be compared with Figure 3-12 illustrating the mean wave period from the ERA5 model data.

And Figure 3-13 presents a histogram of the values of the uncertainty. The values are essentially between 4 and 12 cm, which is consistent with [**RD 9**].

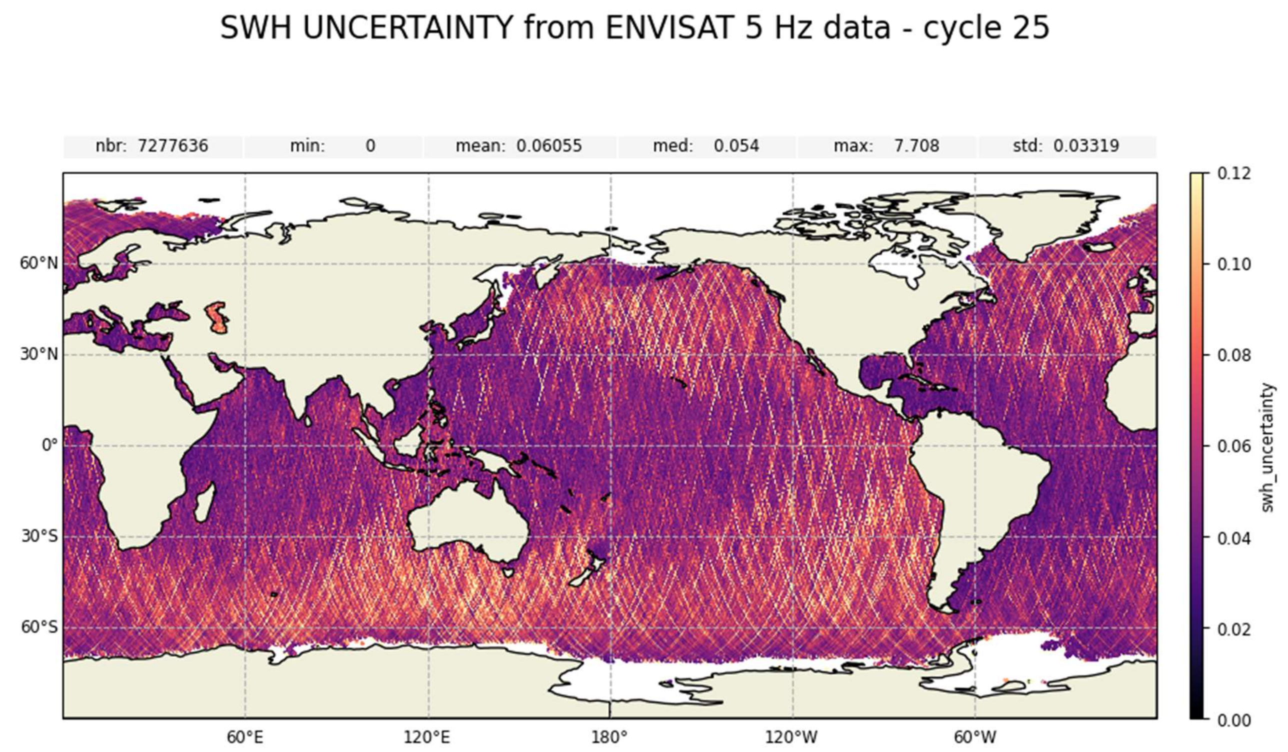

Figure 3-11 – SWH UNCERTAINTY field (raw data) from cycle 25 of ENVISAT data.

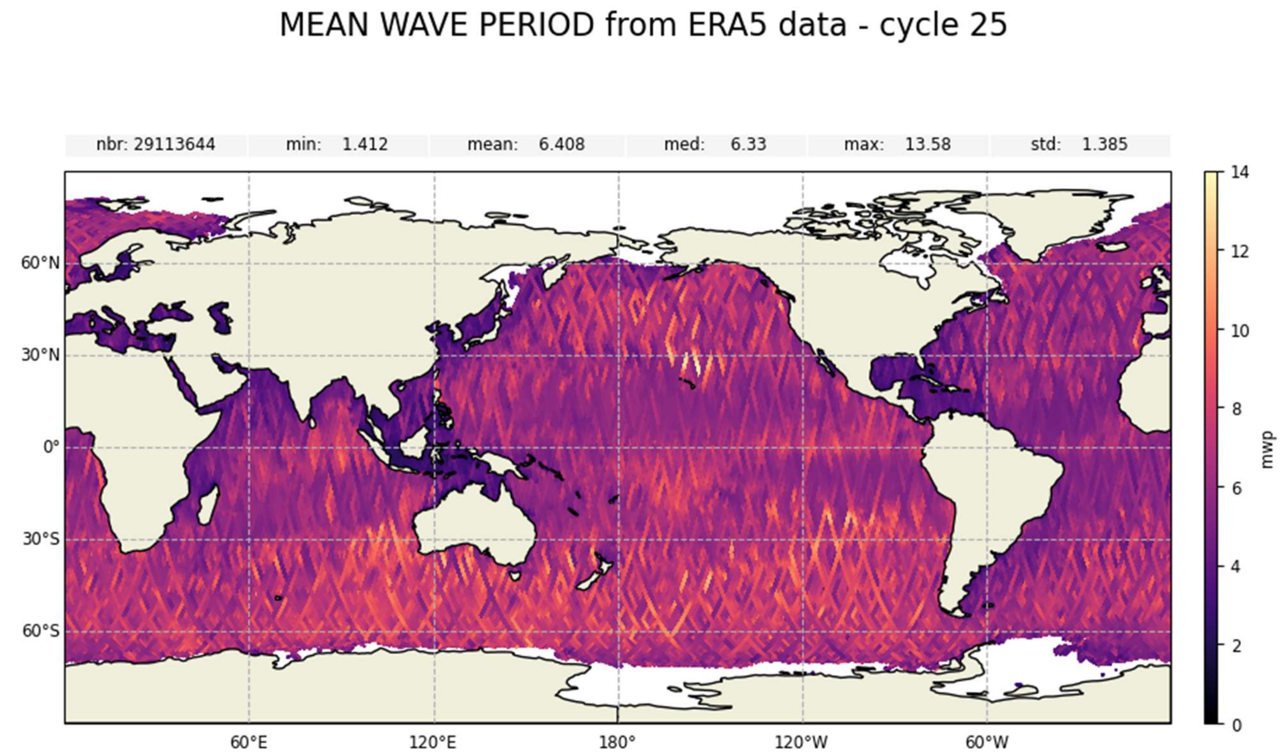

Figure 3-12 – Mean Wave Period from ERA5 Model

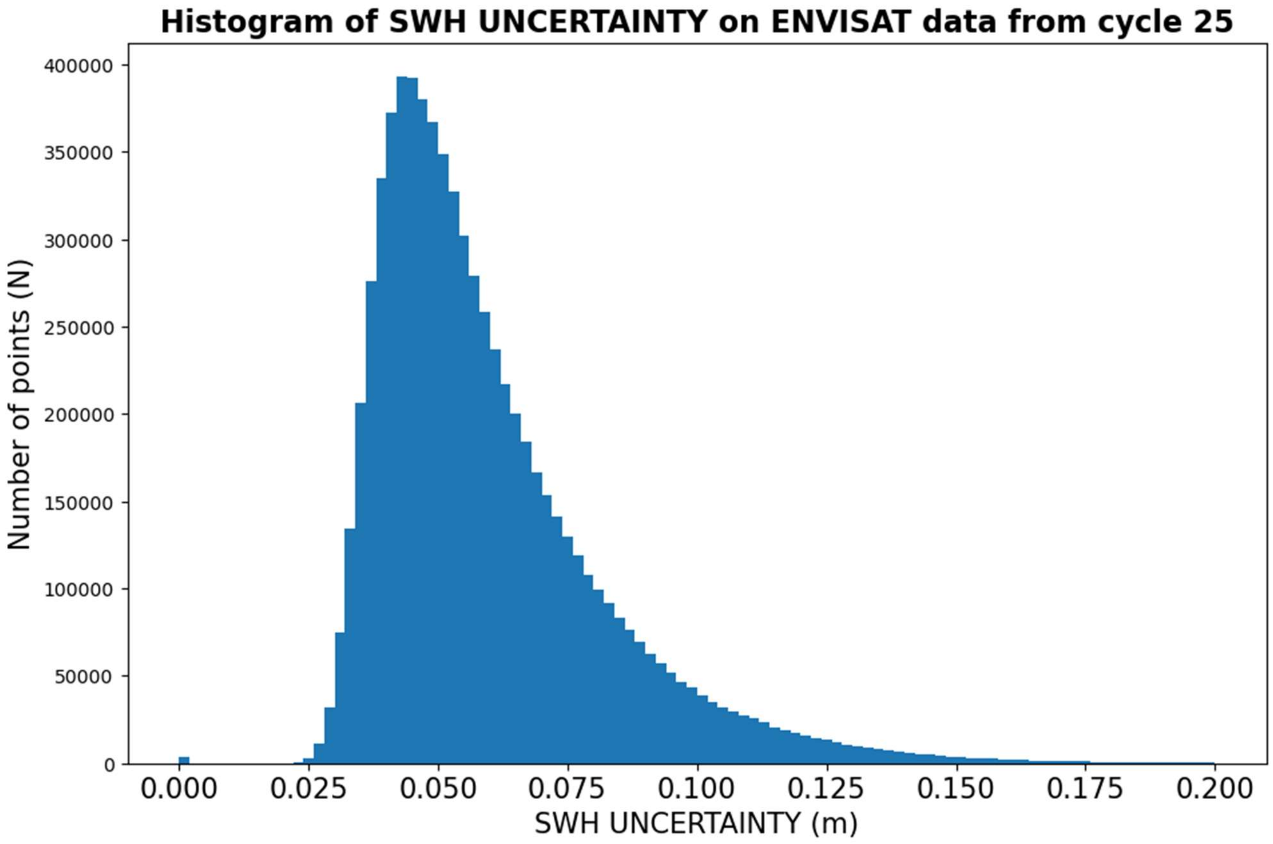

Figure 3-13 – Histogram of SWH uncertainties over cycle 25 of ENVISAT data.

More details on how this uncertainty has been computed are available in the Uncertainty Characterization Report [D-5-02] and the Detailed Processing Model Document [D-2-01].

ERS-1 (cycle 153) and ERS-2 (cycle 40)

Spectral Analysis:

As for ENVISAT data, a spectral analysis was performed on one cycle (35 days) from ERS-1 and ERS-2 data. Results of this spectral analysis have been synthetised in

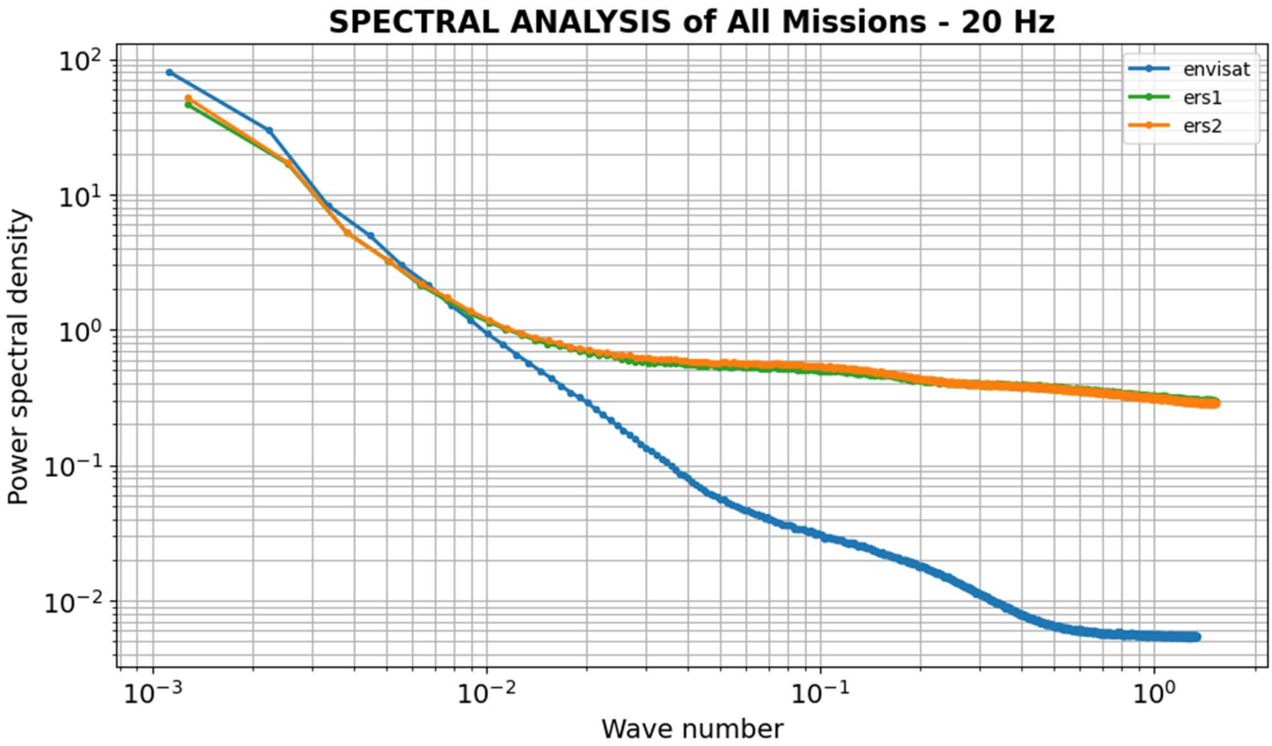

Figure *3-14* and Figure 3-15.

Performances obtained with ERS-1 and ERS-2 missions' data are far lower than performances obtained with ENVISAT data. This comes from the difficulty to perform a High Frequency Adjustment (HFA) correction on ERS data. This step was not computed and the noise in ERS data before any computation of the EMD filter is higher than the noise in ENVISAT data.

The speckle noise is so high that the spectral bump at 10 km is almost completely masked. The EMD filter, used to remove a periodic signal (typically the 10 km spectral bump) is far less efficient in such a situation.

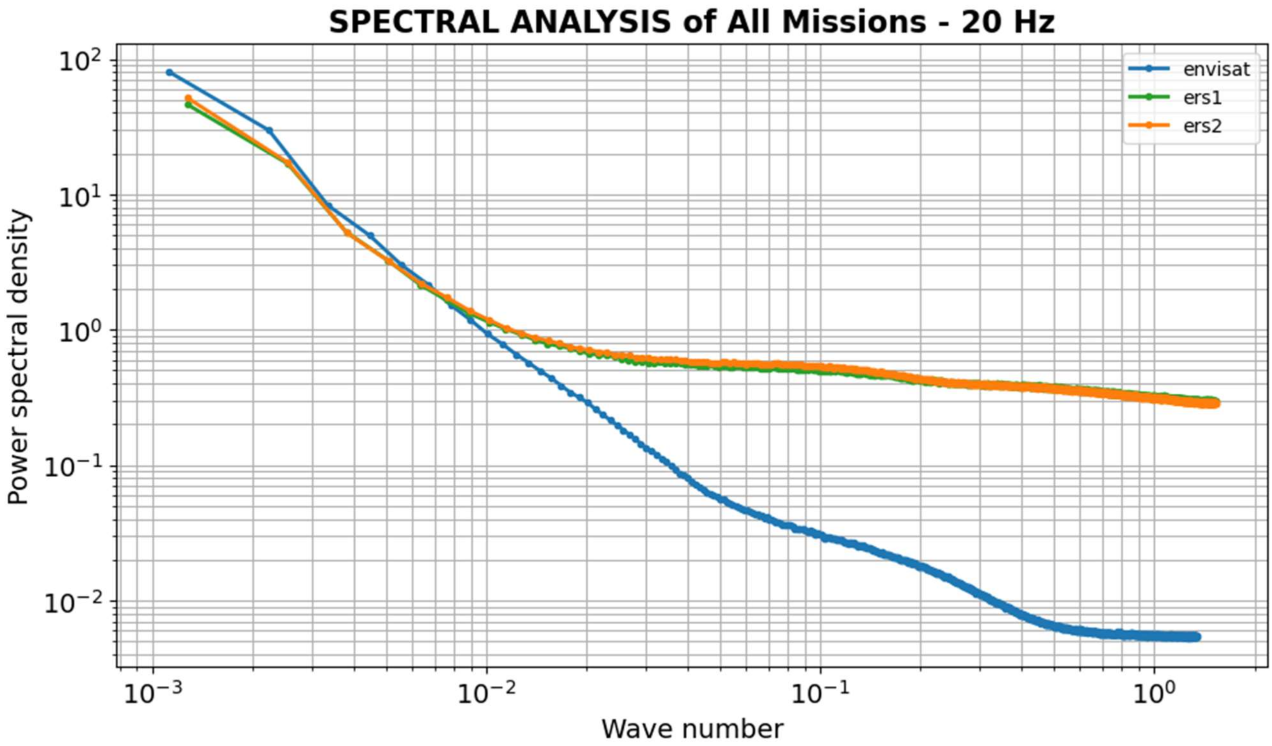

Figure 3-14 – Spectral analysis of 20 Hz data from ENVISAT; ERS-1 and ERS-2 missions over one cycle (35 days)

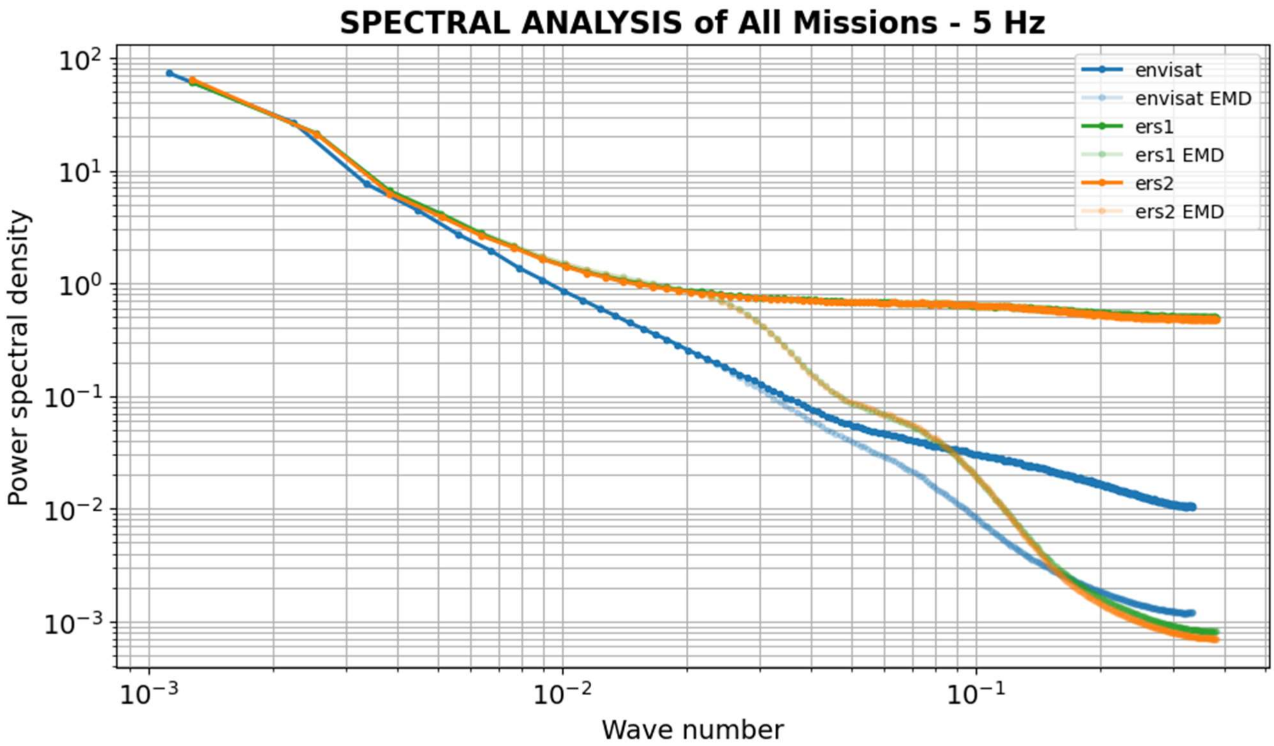

Figure 3-15 – Spectral analysis of 5 Hz data with and without the computation of the EMD filter from ENVISAT; ERS-1 and ERS-2 missions over one cycle (35 days)

<u>Uncertainties:</u>

In this last sub section, results obtained with the computation of the SWH uncertainty from ERS-1 and ERS-2 5 Hz data are presented.ERS-1 and ERS-2 SWH filtered and unfiltered data have similar spectral behavior, and so are their associated uncertainty.

Figure 3-16 and Figure 3-17 show a cartography of the uncertainty from SWH filtered data of cycle 153 from ERS-1 and cycle 40 from ERS-2 missions.

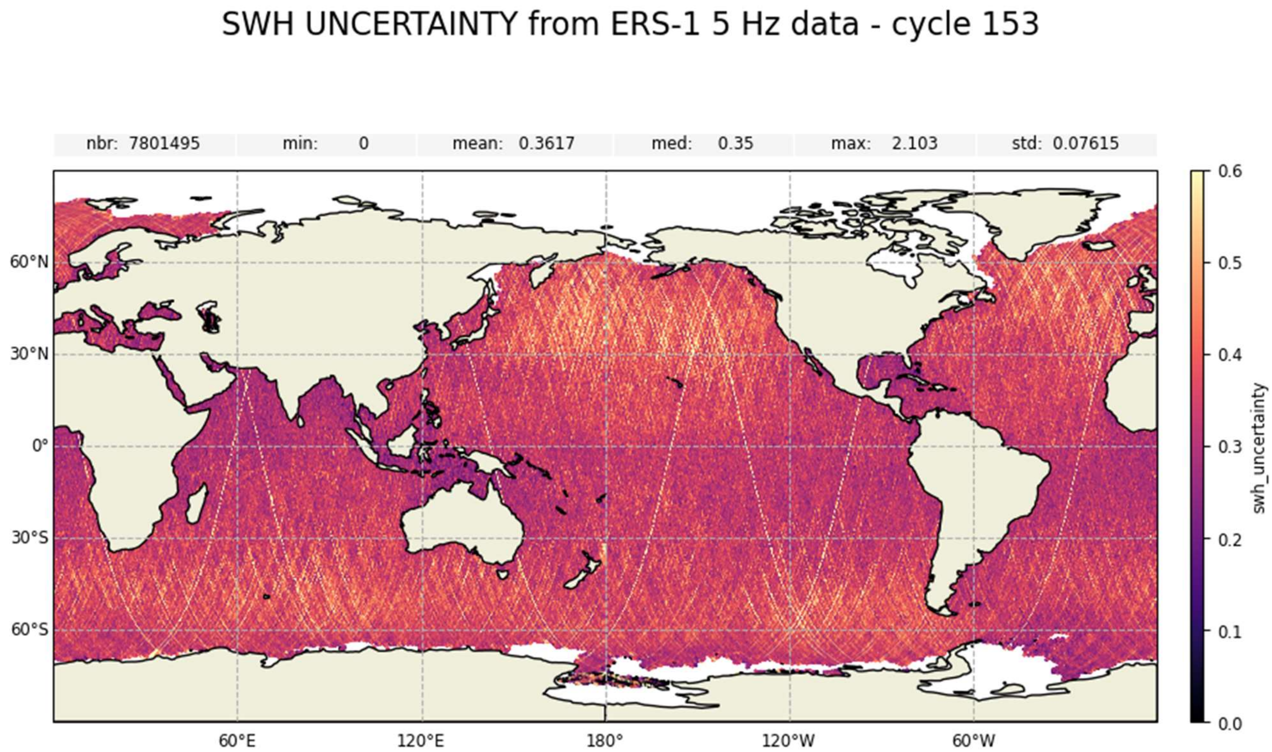

Figure 3-16– SWH uncertainty from cycle 153 of ERS-1 data

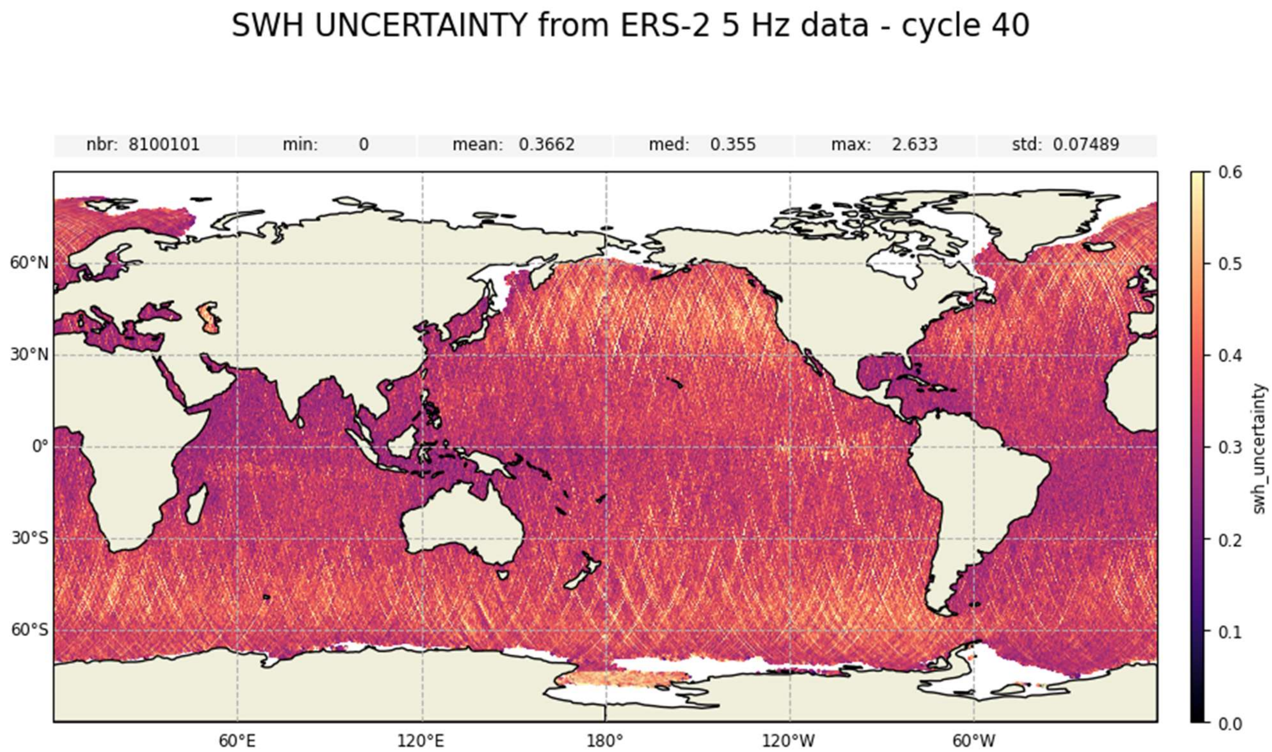

Figure 3-17– SWH uncertainty from cycle 40 of ERS-2 data

Global geographical structures are similar to those obtained with ENVISAT uncertainties. As expected, structures of wave groups are less enhanced than in ENVISAT data. The reason is visible in the spectral analysis. The speckle noise plateau is far higher in ERS data and the spectral bump around 10 km is hidden by this high noise level. Therefore, the wave groups signal is less significant in the residual between filtered and un-filtered signal.

Finally, Figure 3-18 and Figure 3-19 show a histogram of this uncertainty during cycle 153 from ERS-1 data and during cycle 40 from ERS-2 data.

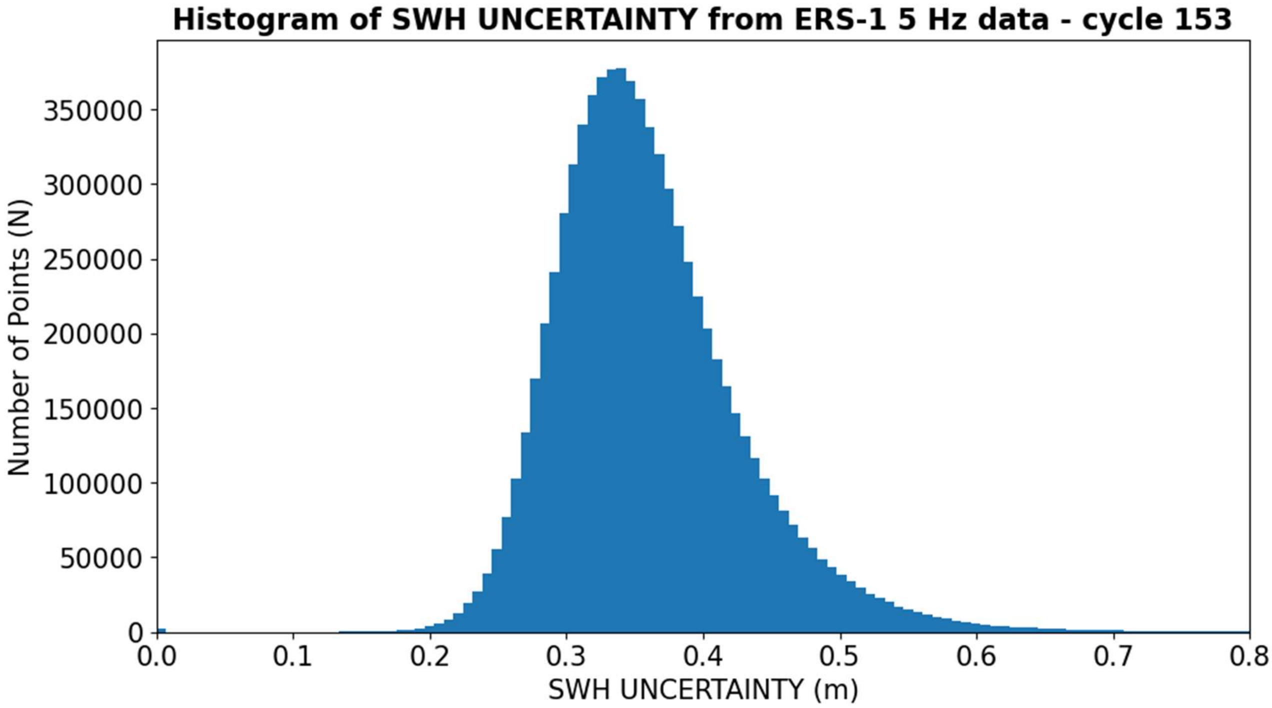

Figure 3-18– Histogram of SWH uncertainty from cycle 153 of ERS-1 data

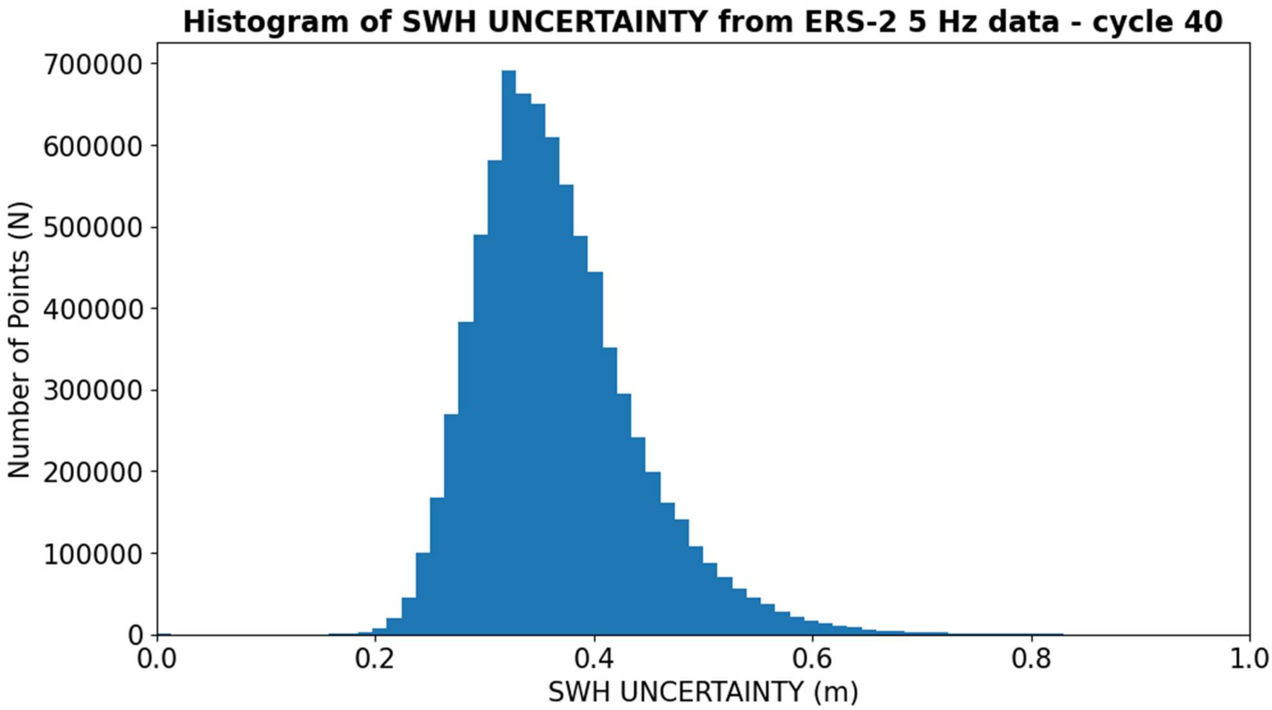

Figure 3-19– Histogram of SWH uncertainty from cycle 40 of ERS-2 data

3.2.4 Validation over the whole period

This last sub section is dedicated to long term validation on SWH, cross calibration between missions and uncertainties.

Calibration of ERS-1 and ERS-2 data:

The method to obtain a consistent time series of Significant Wave Height (SWH) data over the whole period is detailed in the FDR4LT Detailed Processing Model document [D-2-01].

The results of the calibration step are detailed in the following section.

ERS-2 and ENVISAT:

As indicated in the FDR4LT Detailed Processing Model, the calibration between ERS-2 and ENVISAT data was performed using crossover points.

Figure 3-20 and Figure 3-21 represent differences of SWH between ERS-2 and ENVISAT data at crossover points between 2002 June and 2003 May. When we look only at the crossover points, the calibration succeeded reduce the bias between both missions.

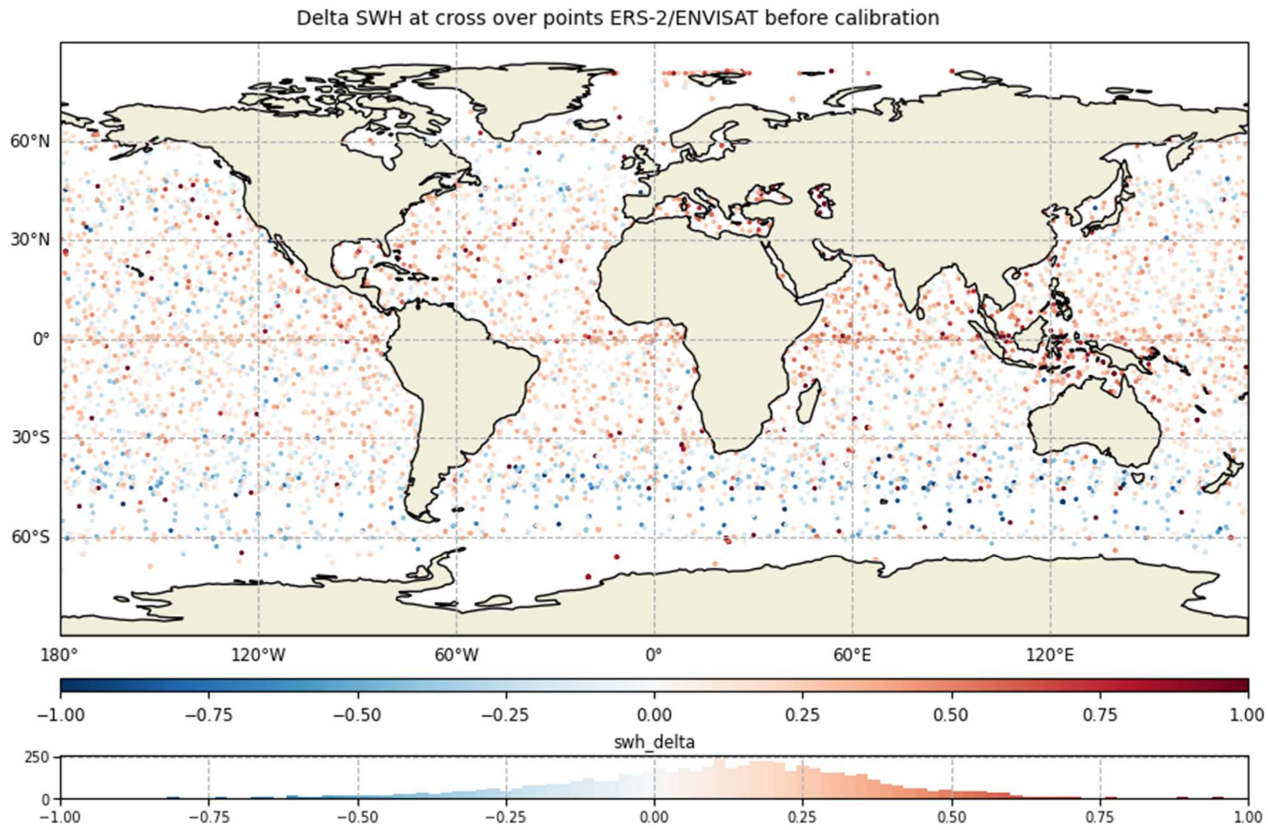

Figure 3-20– Differences of SWH at crossover points between ERS-2 and ENVISAT data before the calibration was performed.

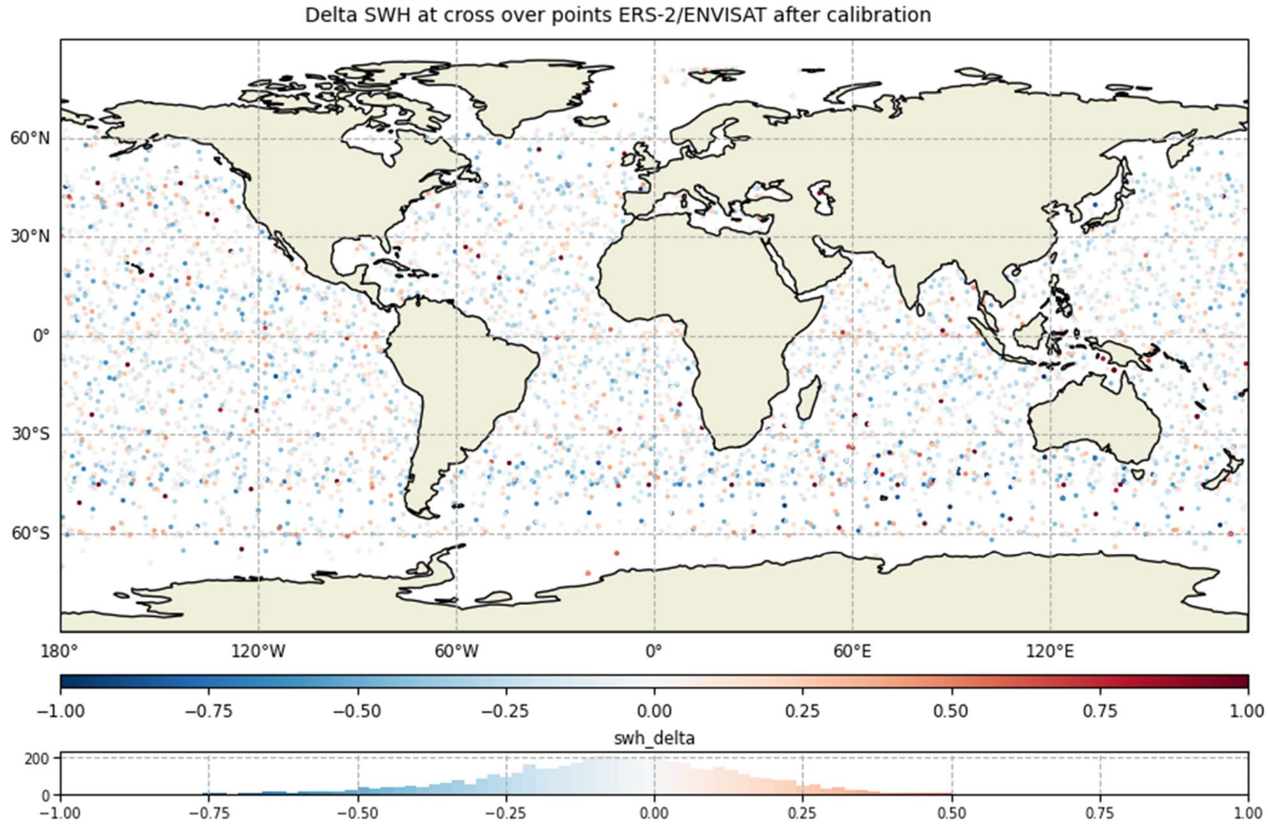

Figure 3-21– Differences of SWH at crossover points between ERS-2 and ENVISAT data after the correction was performed.

The result on the long-term monitoring of SWH data is given in Figure *3-22*.

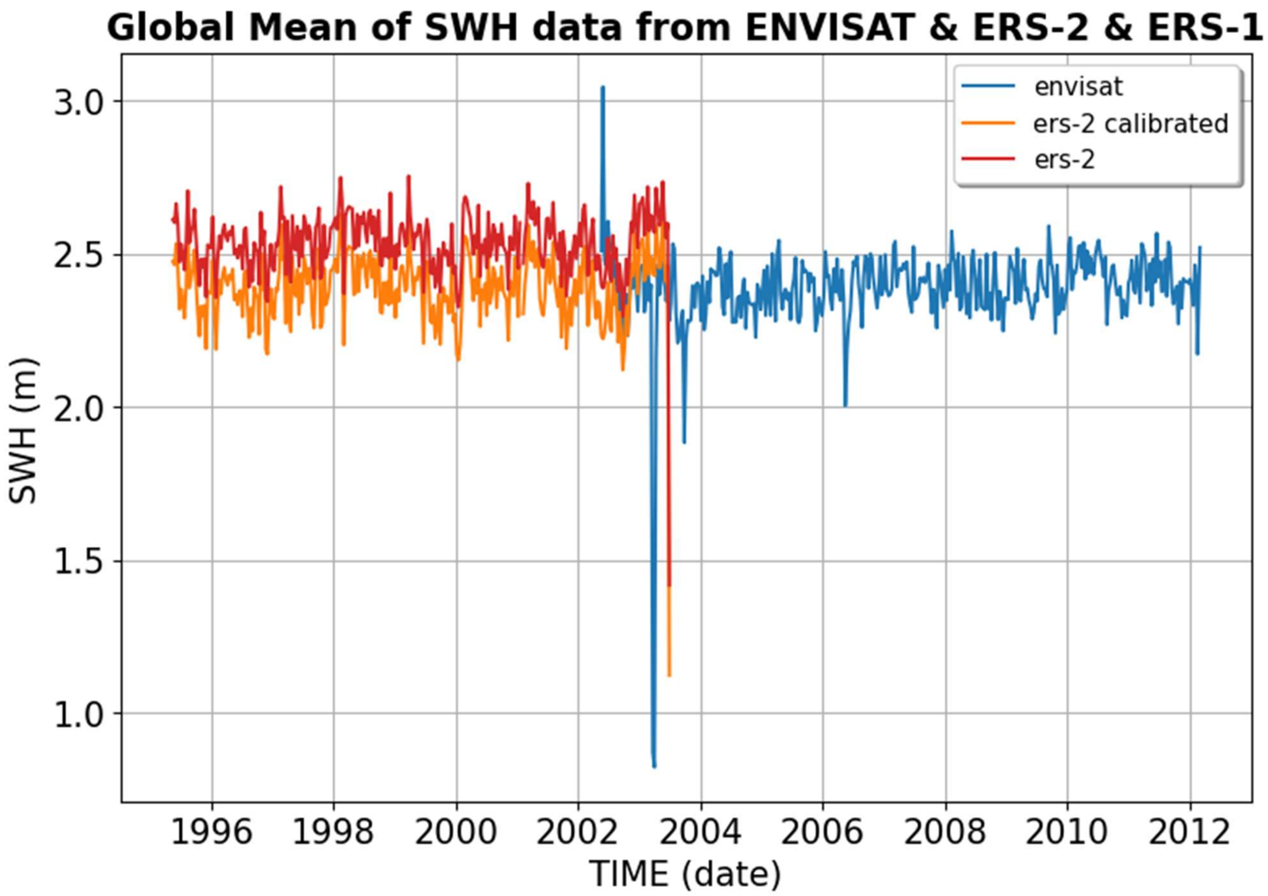

Figure 3-22– Time series of SWH from ENVISAT and ERS-2 data; before and after the calibration was performed.

The mean of ENVISAT data is 2.398 m. The mean of ERS-2 data before any calibration was 2.535 m, and the relative error between both was 5 %.

After the calibration was performed, the mean of ERS-2 data is 2.388 m, and the relative error is 0.4 %.

The calibration of ERS-2 data with respect to ENVISAT data succeeded.

ERS-1 and ERS-2:

As indicated in the FDR4ALT Detailed Processing Model, the calibration between ERS-1 and ERS-2 was more difficult to implement as there are no crossover points with a time delta lower than three hours.

The ERA5 model was used as an intermediate variable to compare both ERS-1 and ERS-2 data. Differences between ERS-1 and ERA5 data should be the same as differences between ERS-2 and ERA5 data.

The only diagnosis to evaluate the calibration between ERS-1 and ERS-2 data is the comparison of time series. In the following figure (Figure 3-23), time series of ERS-2 calibrated data and ERS-1 data (before and after the calibration was performed) are represented:

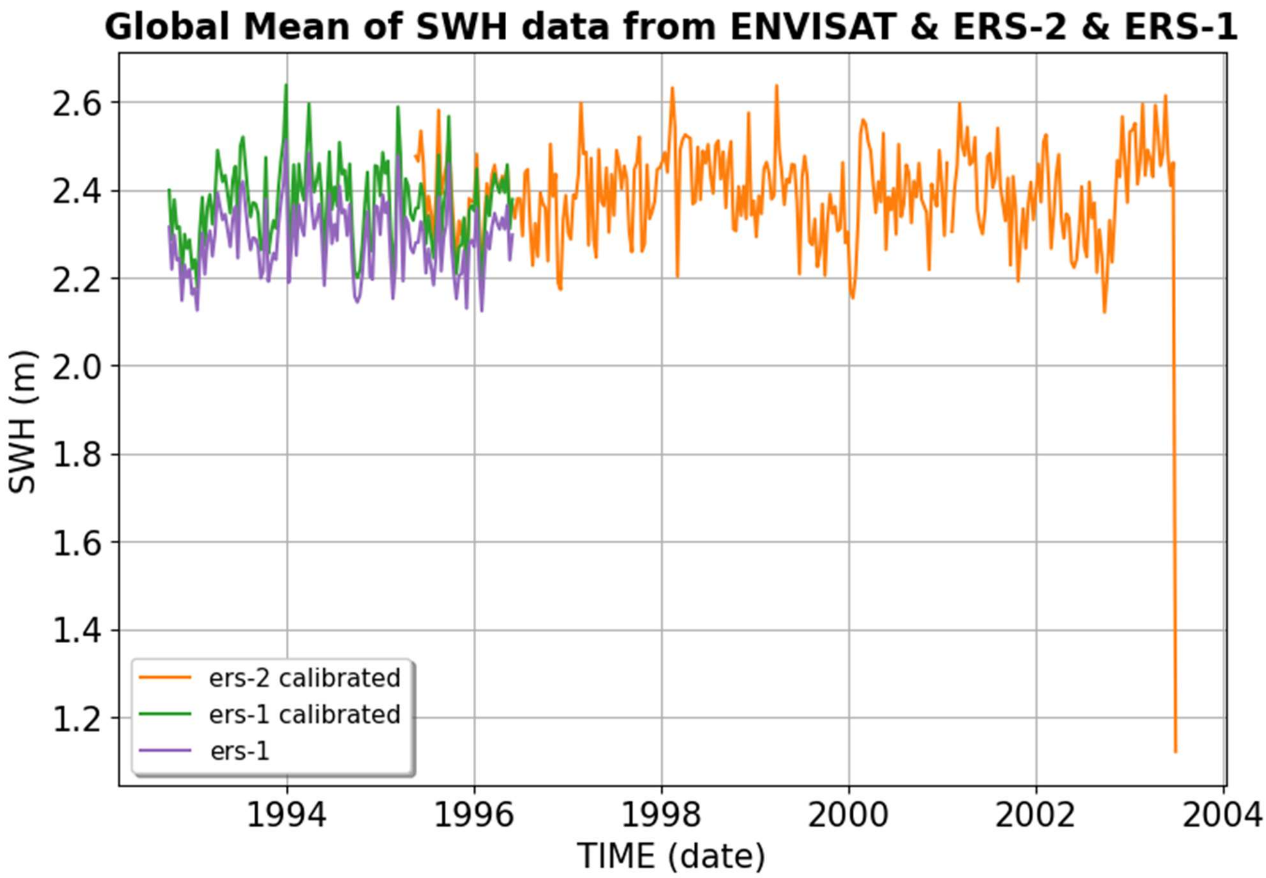

Figure 3-23– Time series of SWH from ERS-2 and ERS-1 data; before and after the calibration was performed.

The mean of ERS-2 data is 2.388 m. The mean of ERS-1 data before any calibration was 2.286 m, and the relative error between both was 4 %.

After the calibration was performed, the mean of ERS-1 data is 2.366 m, and the relative error is 0.9 %.

The calibration of ERS-1 data with respect to ERS-2 data succeeded.

➔ **Final result:**

The last diagnosis to evaluate the performances of FDR4ALT Ocean Waves TDP products is a long-term analysis computed with the method used to compute the global mean sea level. Another way to confirm the efficiency of the calibration between all three missions was to compute this global evolution of the Significant Wave Height over the whole time period before and after the calibration of ERS-1 and ERS-2 data was applied. The results are presented in Figure 3-24 and Figure 3-25.

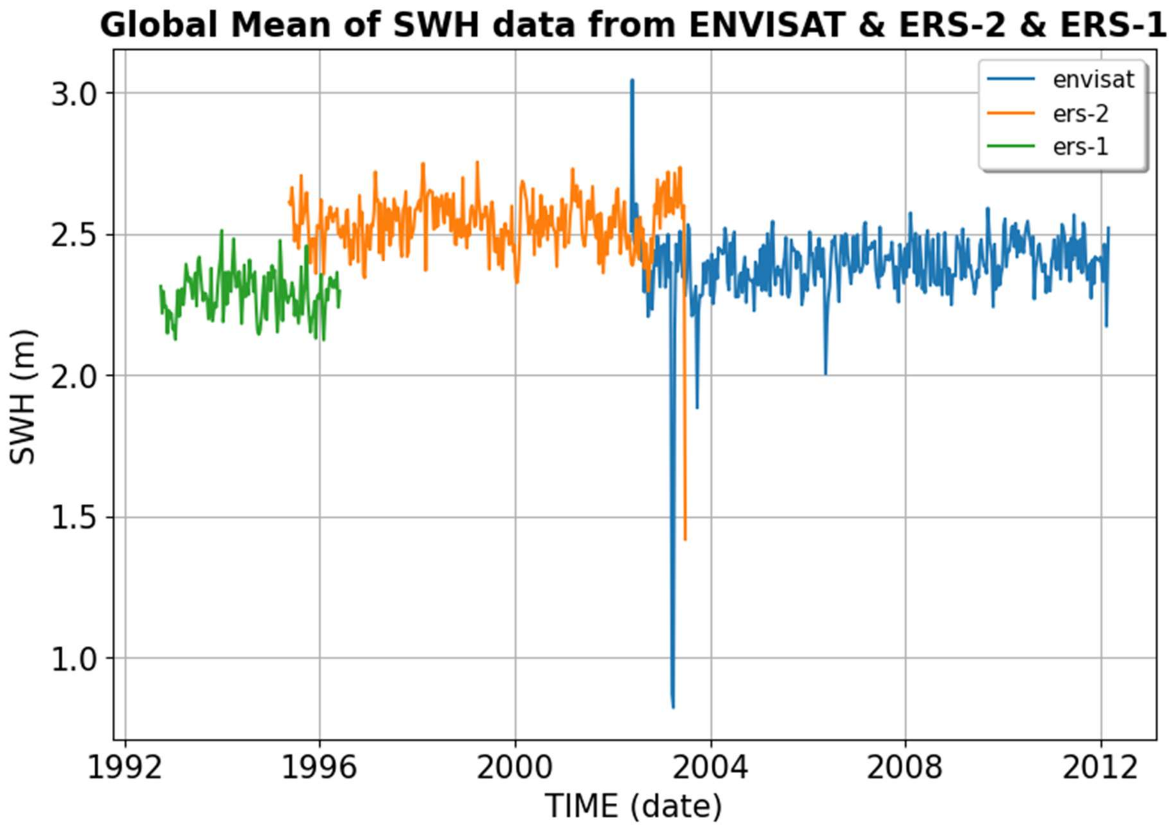

Figure 3-24 – Evolution of the mean SWH value from ENVISAT/ERS-2/ERS-1 data over the whole time period before calibration

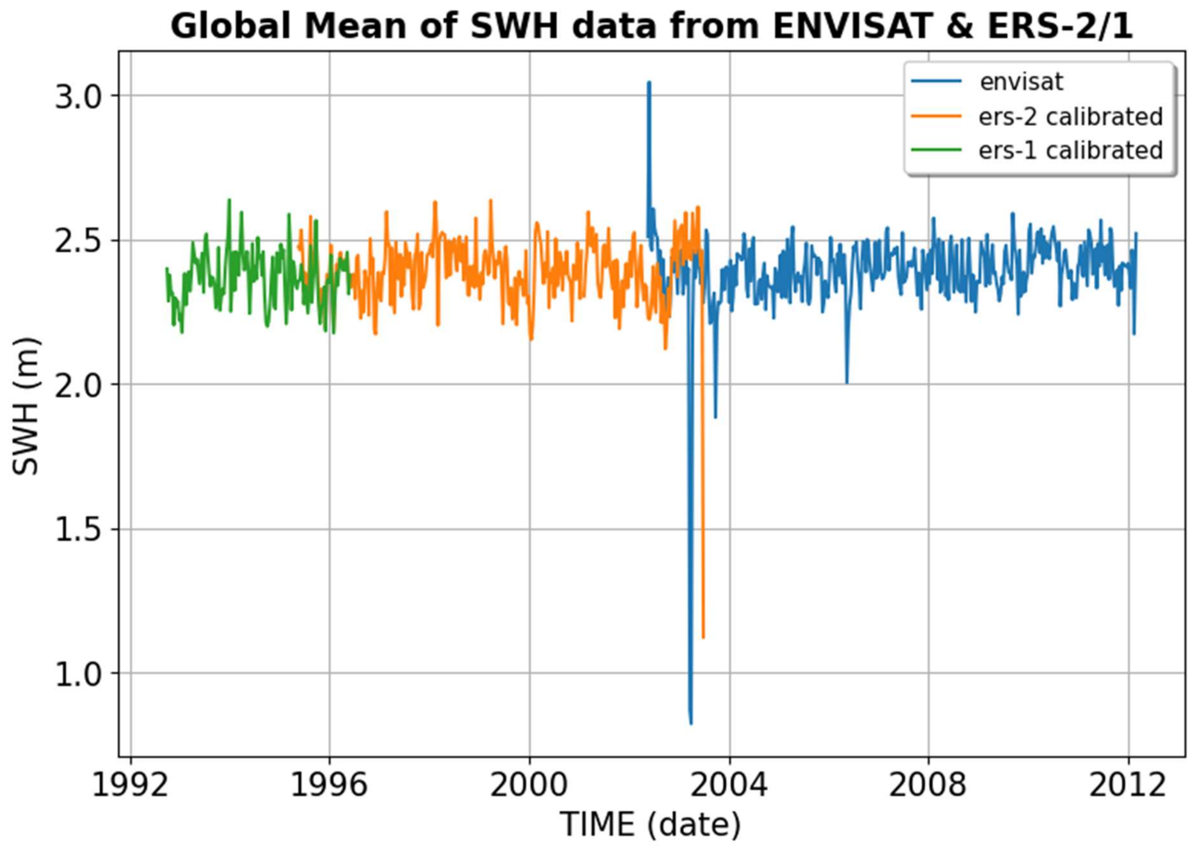

*Figure 3-25 – Evolution of the mean SWH value from ENVISAT/ERS-2/ERS-1 data over the whole time period after calibration*The

The FDR4ALT project led to an example of a long term (20 years) monitoring of SWH mean values using three altimetry missions. It illustrates the impact and the interest of the computation of an efficient calibration between satellite missions.

The global SWH value is quite stable as the mean of ENVISAT data is 2.398 m, the mean of ERS-2 data is 2.388 m and the mean of ERS-1 data is 2.366 m.

The calibration is really efficient as the relative error between ENVISAT and ERS-2 data is 0.4 % (5 % before calibration), the relative error between ERS-2 and ERS-1 data is 0.9 % (4 % before calibration) and the relative error between ENVISAT and ERS-1 data is 1.3 % (4.6 % before calibration).

This diagnosis illustrates a great stability in SWH values over time. This conclusion is about global scales: it seems there is no global trend in SWH values as there is in Sea Level values. The last section is about regional scales of the evolution of SWH values.

Global SWH results:

The validation of the content of SWH field in FDR4ALT products over the whole time period, several diagnoses was performed.

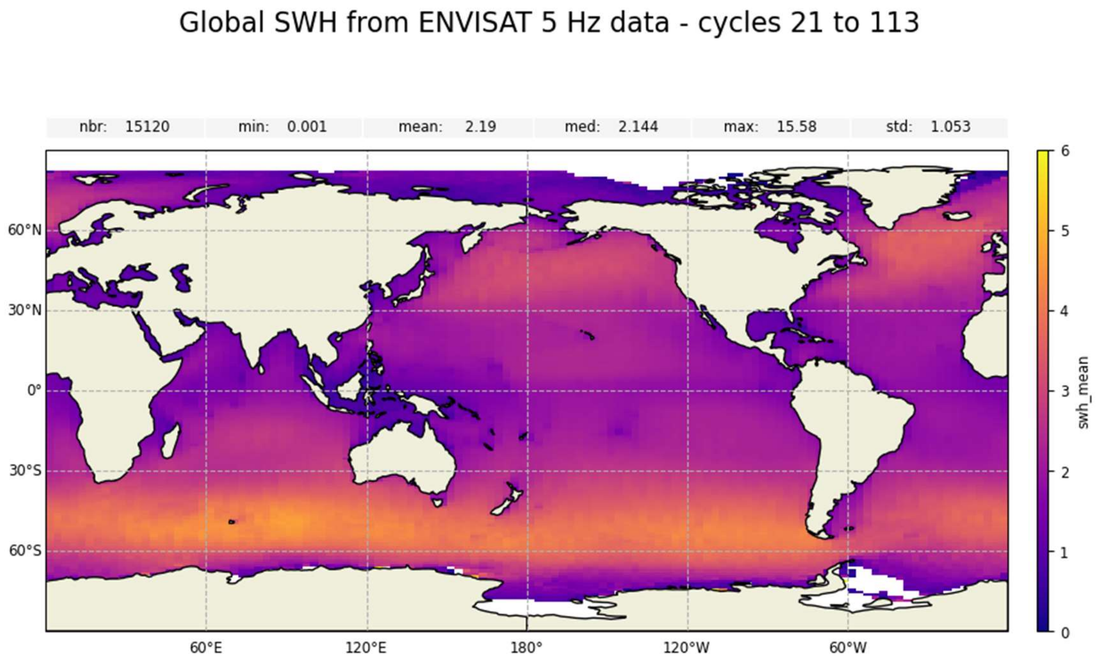

Figure 3-26, Figure 3-27 and Figure 3-28 are global cartographies of SWH values from ENVISAT, ERS-2 and ERS-1 missions over the whole period of each mission. The colour scale is the same in all three plots, so the comparison can be direct between results obtained with different missions.

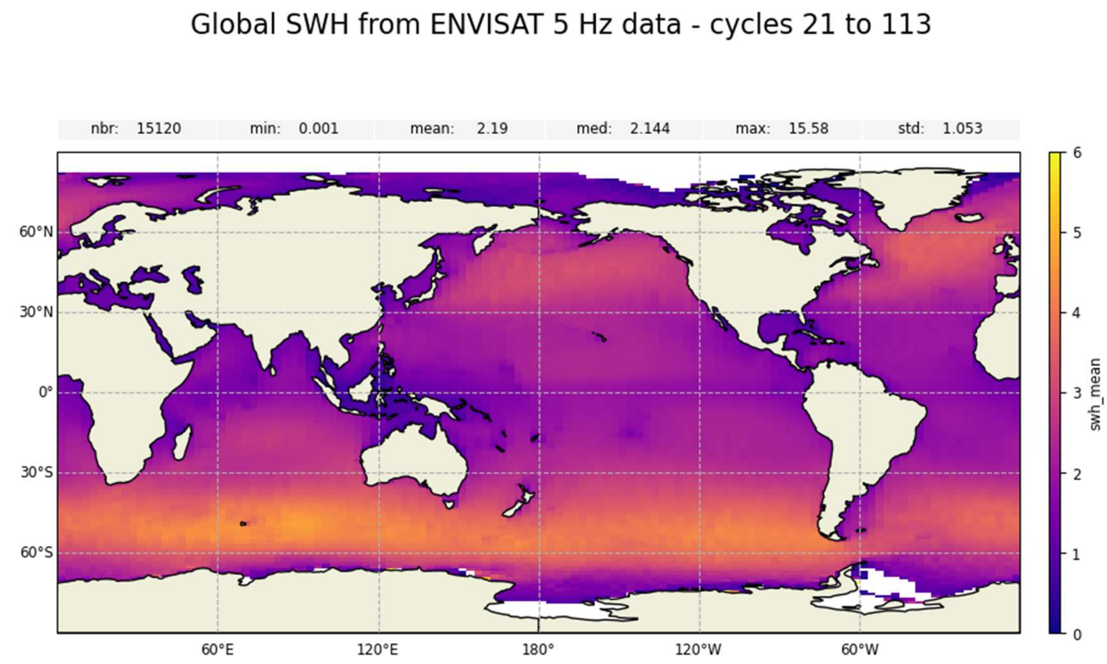

Figure 3-26 : Mean of SWH values from ENVISAT data per geographical boxes (1° x 3°) from cycle 21 to 113

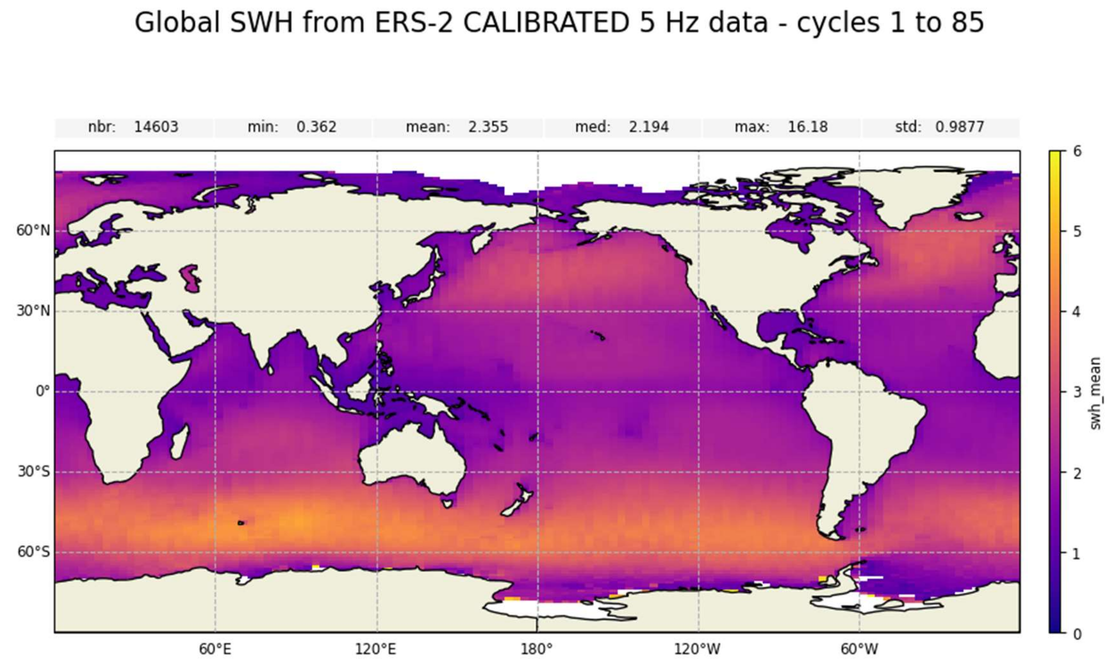

Figure 3-27: Mean of SWH values from calibrated ERS-2 data per geographical boxes (1° x 3°) from cycle 1 to 85

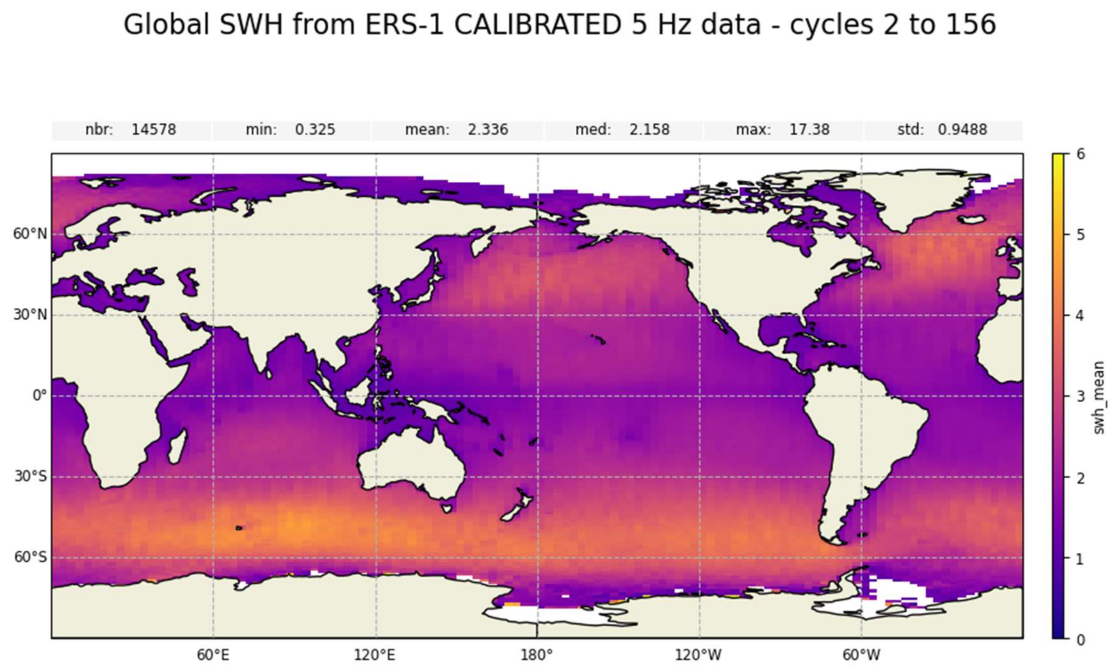

Figure 3-28 ;Mean of SWH values from calibrated ERS-1 data per geographical boxes (1° x 3°) from cycle 2 to 156

To evaluate the regional performances of the calibration between missions, a difference of those cartographies has been computed before and after the calibration was applied to ERS-1 and ERS-2 data. Results of those differences are presented in Figure 3-29, Figure 3-30, Figure 3-31 and Figure 3-32. The effect of the calibration can be observed in all areas and for all values of significant wave height.

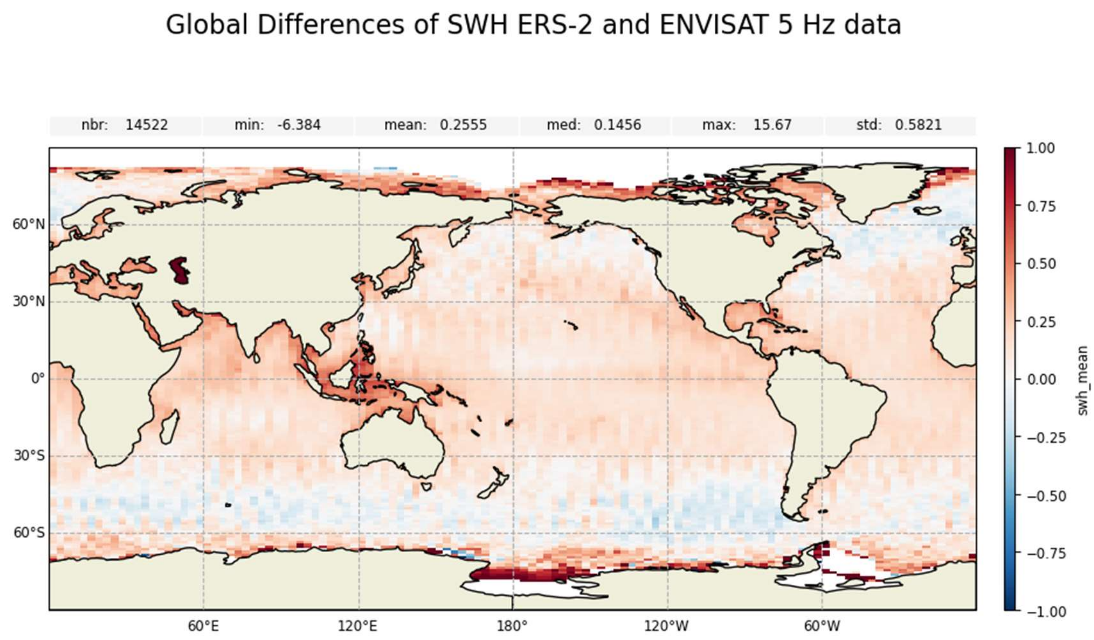

Figure 3-29 – Differences of Mean SWH between ENVISAT and ERS-2 data before calibration

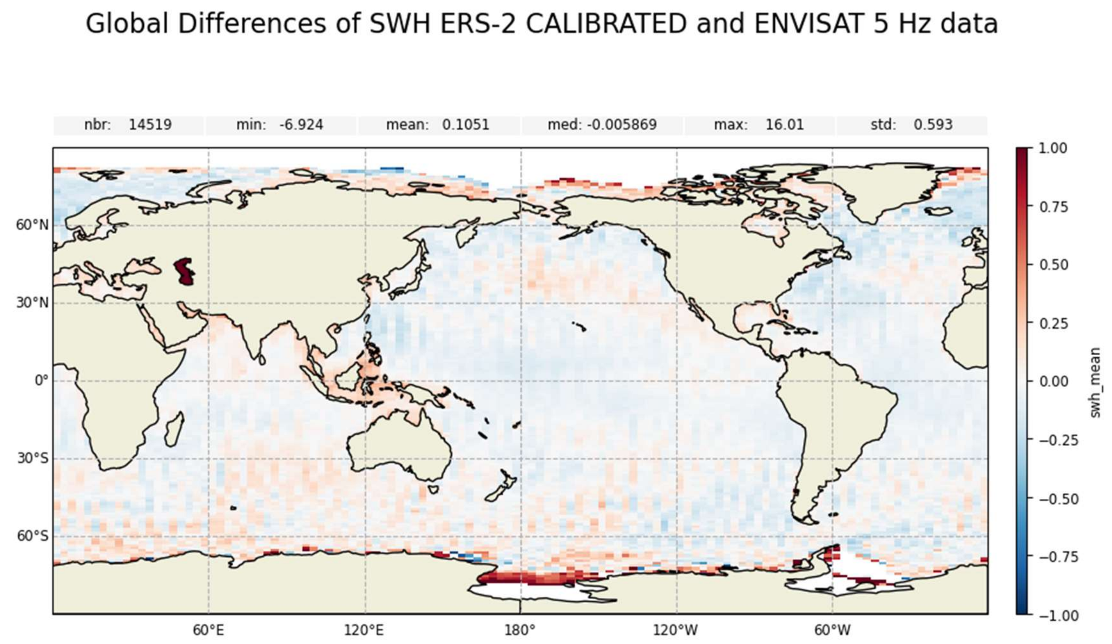

Figure 3-30 – Differences of Mean SWH between ENVISAT and ERS-2 data after calibration

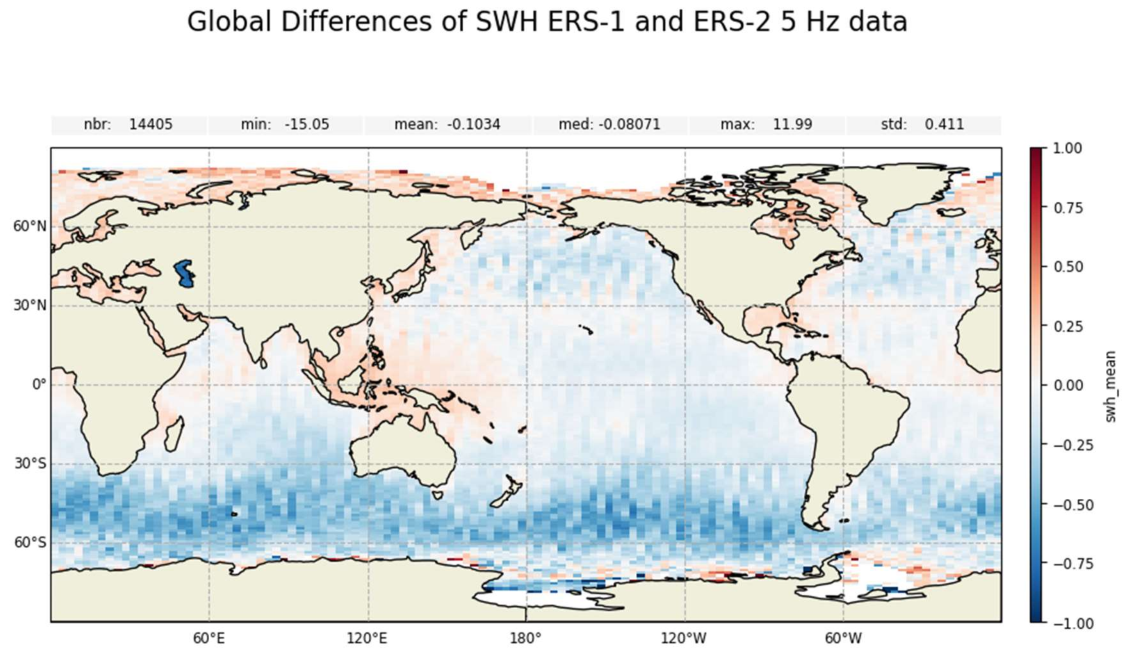

Figure 3-31 – Differences of Mean SWH between ERS-2 and ERS-1 data before calibration

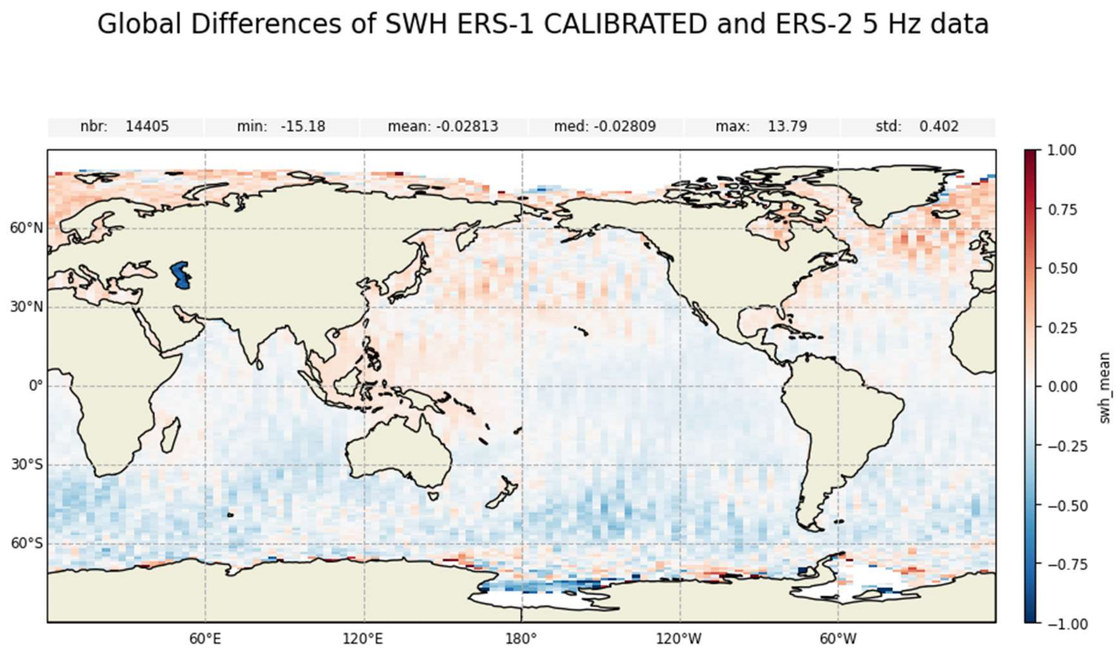

Figure 3-32 – Differences of Mean SWH between ERS-2 and ERS-1 data after calibration

Regional Trend:

After a global analysis of SWH values, this section presents the regional trend over the whole period of the ENVISAT mission, the value of significant wave height averaged per boxes (1° x 3°). It seems that there is an increase of the averaged SWH in a lot of areas (but the formal uncertainty is really high, so the result should be moderated). But an interesting observation is that some areas seem to present a decrease of this averaged SWH (still with a big uncertainty).

Results obtained with FDR4ALT ENVISAT new dataset seem to be consistent with results presented by the CCI Sea State project in [**RD 16**].

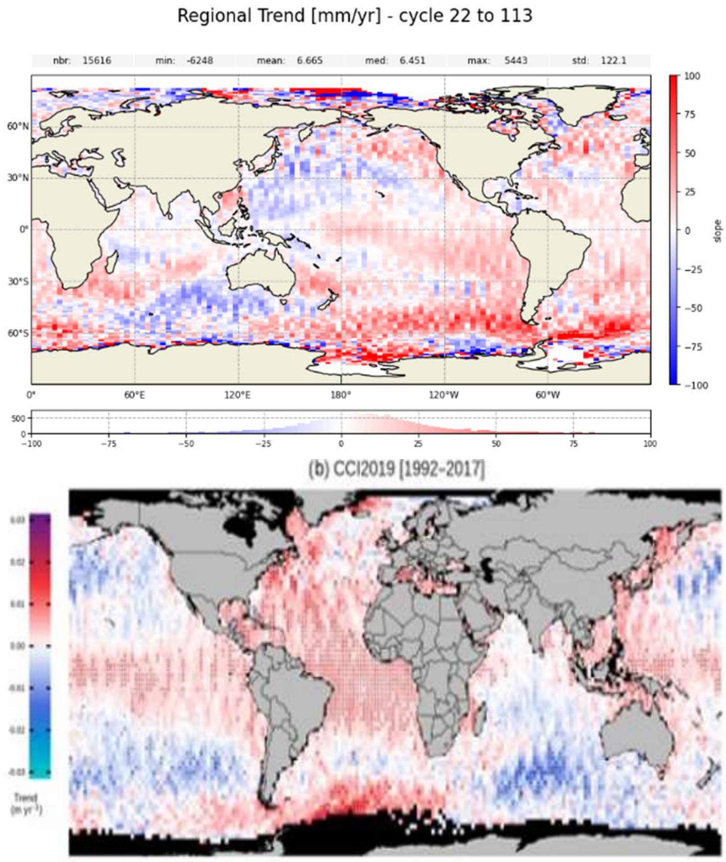

Figure 3-33 – Regional trend of the evolution of the mean SWH value from ENVISAT data per geographical boxes (1° x 3°) (left) and regional trend of the mean swh values over 25 years (obtained by CCI Sea State) (right)

Uncertainties:

In the following plots (Figure 3-34, Figure 3-35 and Figure 3-36) are presented the mean of SWH uncertainty values by geographical boxes (1°x3°) during the whole period of mission. It confirms the regional structures observed over one cycle in the previous section for ENVISAT data. Uncertainties of ERS-1/2 data are mostly correlated with SWH values. It is explained by the fact that the spectral bump is masked by the high level of noise in ERS data.

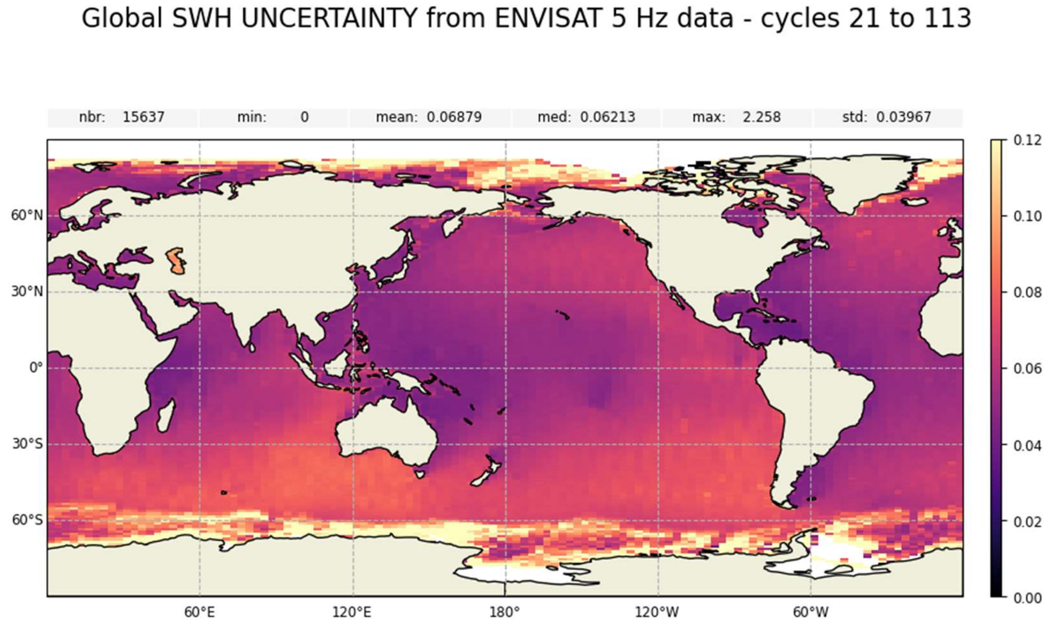

Figure 3-34 – Mean of SWH uncertainty values from ENVISAT data from cycle 21 to 113

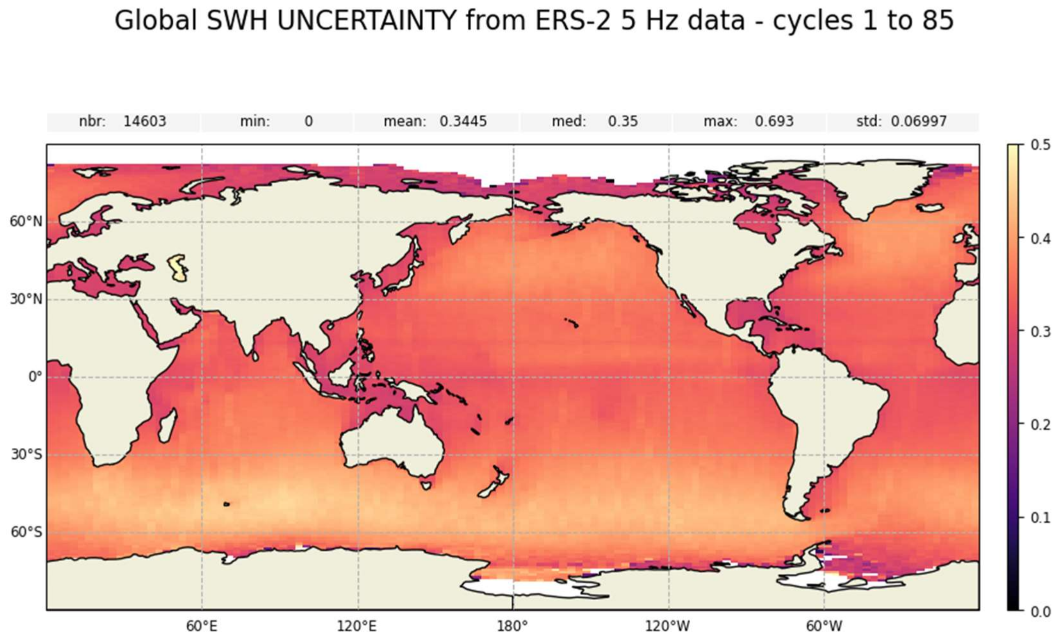

Figure 3-35 – Mean of SWH uncertainty values from ERS-2 data from cycle 1 to 85

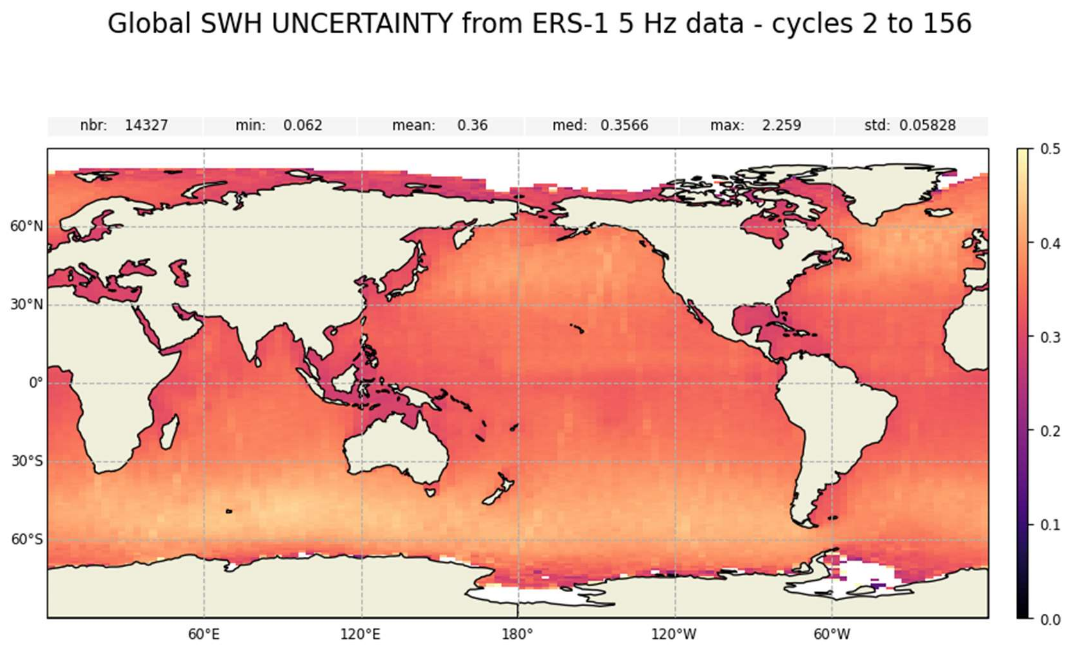

Figure 3-36 – Mean of SWH uncertainty values from ERS-1 data from cycle 2 to 156

The same long-term analysis was performed on this uncertainty field than the one presented in. The result for the evolution of those uncertainties from each mission at global scale is presented in. A great consistency is observed between uncertainties from ERS-1 and ERS-2 data. Uncertainties from ENVISAT are far lower as it was observed from cartographies.

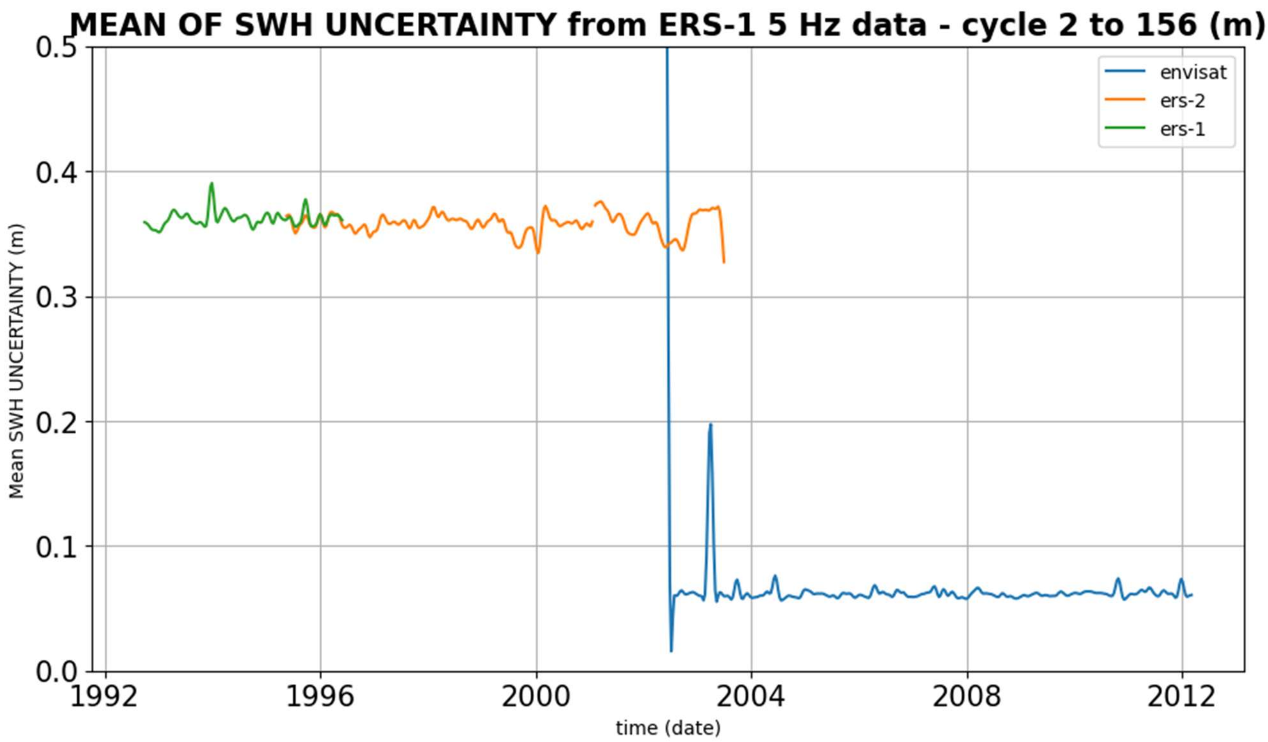

Figure 3-37 – Evolution of the mean SWH UNCERTAINTY from ENVISAT data over the whole time period with associated trend

The last diagnosis presented in is the regional trend of this uncertainty.

It can be observed that this uncertainty seems to grow with time in a lot of regions. This result is interesting because this uncertainty is a measure of the variability removed by the EMD filter, itself related to the wave period. This variability is the one related to the sea state and the spectral bump around 10 km. It will be interesting to carry out further investigation on this result.

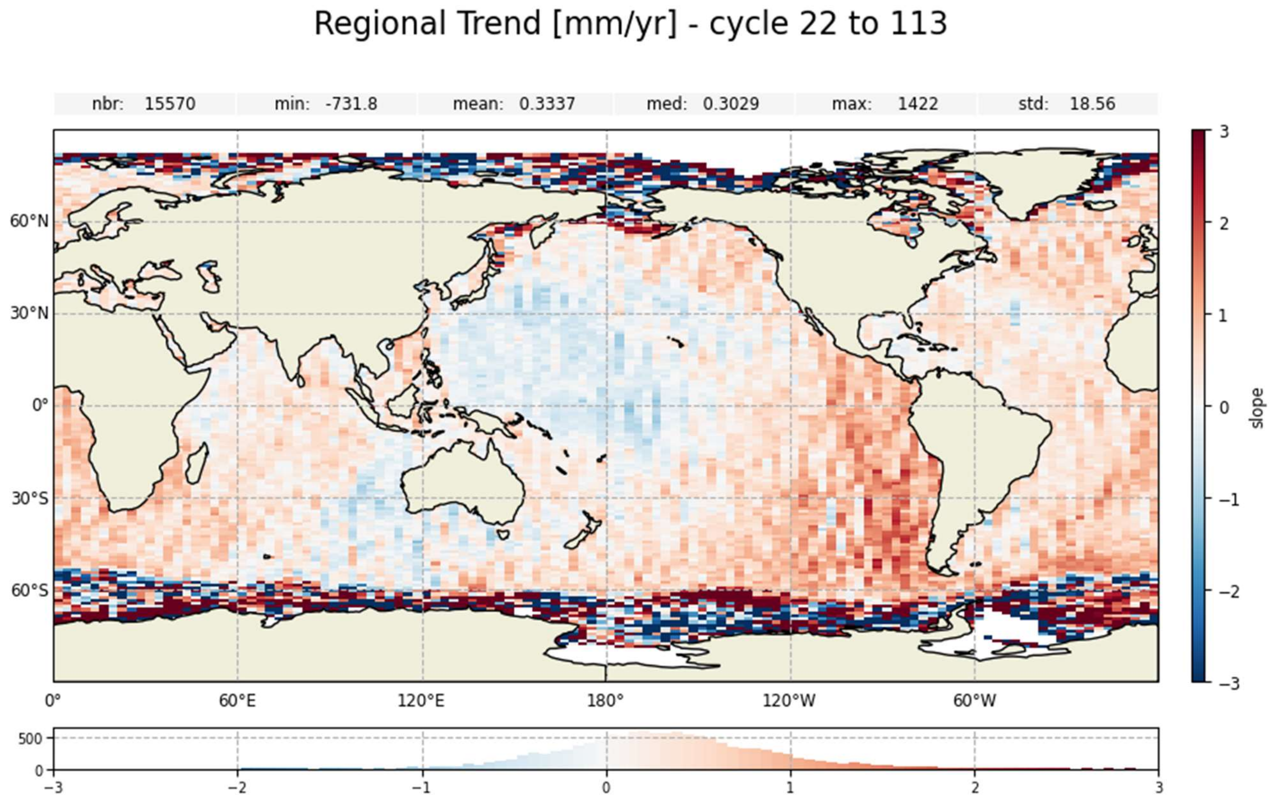

Figure 3-38 – Regional trend of the evolution of uncertainties of ENVISAT data per geographical boxes (1°x3°) from cycle 22 to 113

3.3 Conclusion and remarks

The important results of this section can be summarized in four points:

- ✓ The FDR4ALT OW TDP delivers good quality data of SWH on open ocean.
- ✓ They present a great added value both in spectral content and the approach to the coast.
- ✓ Performances obtained with FDR4ALT products are better than those obtained with the current CCI Sea State dataset and the previous version of ENVISAT data.
- ✓ A filtering is applied to reach short scale variability with a filtering of an effect related to the system of measurement over correlated areas and the residual is given as an estimate of the measure uncertainty.

FDR4ALT OW TDP data are ready to be published for users as a new reference for ENVISAT missions.

A first version of uncertainty field is provided and will possibly be improved based on the users' feedback (also within the CMEMS WAVE-TAC forum).

3.4 Reference documents

RD 1	Sepulveda H. H., Queffeulou P. and Ardhuin F. (2015): Assessment of SARAL AltiKa wave height measurements relative to buoy, Jason-2 and Cryosat-2 data. Marine Geodesy, 38 (S1),449-465, doi:

	10.1080/01490419.2014.1000470. Queffeulou P. (2016): Validation of Jason-3 altimeter wave height measurements (poster). OSTST meeting, November 1-4, 2016, La Rochelle, France.
RD 2	Queffeulou P. and Croizé-Fillon D. (2017): Global Altimeter SWH Data Set, version 11.4, February 2017. Technical report Ifremer. ftp://ftp.ifremer.fr/ifremer/cersat/products/swath/altimeters/waves/documentation/altimeter_wave_merge__11.4.pdf
RD 3	Tourain C.(1), D. Hauser(2), L. Hermozo(1), R. Rodriguez Suquet(1), P. Schippers(2), L. Aouf(4), A. Dalphinet(4), A. Mouche(5), B. Chapron(5), F. Collard(5), C. Dufour(2), F. Gouillon(1), A. Ollivier(7) , F.Piras(6) ,M. Dalila (6), G. Guitton(5), J-M. Lachiver(1), C. Tison(1) Cal/val phase for the swim instrument onboard cfosat https://hal.archives-ouvertes.fr/hal-03018498/document
RD 4	https://catalogue.marine.copernicus.eu/documents/PUM/CMEMS-WAV-PUM-014-005-006-007.pdf
RD 5	https://www.aviso.altimetry.fr/fileadmin/documents/data/tools/hdbk_L2P_WAVE_S3.pdf
RD 6	https://www.aviso.altimetry.fr/fileadmin/documents/data/tools/SWH_1Hz_CFOSAT_L2P_handbook_SALP.pdf
RD 7	https://climate.esa.int/media/documents/Sea_State_CCI_poster_2020.pdf
RD 8	The Sea State CCI dataset v1 : towards a Sea State Climate Data Record based on satellite observations Guillaume Dodet1 , Jean-François Piolle1 , Yves Quilfen1 , Saleh Abdalla2 , Mickaël Accensi1 , Fabrice Ardhuin1 , Ellis Ash3 , Jean-Raymond Bidlot2 , Christine Gommenginger4 , Gwendal Marechal1 , Marcello Passaro5 , Graham Quartly6 , Justin Stopa7 , Ben Timmermans4 , Ian Young8 , Paolo Cipollini9 , and Craig Donlon10: https://essd.copernicus.org/articles/12/1929/2020/
RD 9	https://seastatecci-ucm.sciencesconf.org/resource/page/id/7
RD 10	Angélique Mélet, Benoit Meyssignac, Rafael Almar, Gonéri Le Cozannet. Under-estimated wave contribution to coastal sea-level rise. *Nature Climate Change*, Nature Publishing Group, 2018, 8 (3), pp.234-239. ⟨10.1038/s41558-018-0088-y⟩. ⟨hal-02860438⟩
RD 11	https://www.aviso.altimetry.fr/fileadmin/documents/calval/validation_report/EN/EnvisatReprocessingReport.pdf
RD 12	Statistics of Ocean Wave Groups K.G. Nolte and F.H. Hsu Paper presented at the Offshore Technology Conference, Houston, Texas, April 1972. Paper Number: OTC-1688-MS https://doi.org/10.4043/1688-MS Published: April 30 1972
RD 13	https://www.frontiersin.org/articles/10.3389/fmars.2019.00124/full
RD 14	DeCarlo et al. 2022 OSTST Small scale wave height variability and wave groups (altimetry.fr)
RD 15	Ollivier et al. 2022 OSTST Microsoft PowerPoint - Pres_DemoProduct_WAVE_5Hz_OSTST2022.pptx (altimetry.fr)
RD 16	https://essd.copernicus.org/articles/12/1929/2020/
RD 17	De Carlo Marine, Fabrice Ardhuin, Annabelle Ollivier, et al. Wave groups and small scale variability of wave heights observed by altimeters. Authorea. February 27, 2023.

Appendix A - FDR4ALT deliverables

The table below lists all FDR4ALT deliverables with their respective ID number and confidentiality level.

Document	ID	Confidentiality Level
Products Requirements & Format Specifications Document	[D-1-01] [D-2-02]	Public
Roadmap & Product Summary Document	[D-1-02]	Project Internal
Data Requirements Document	[D-1-03]	Project Internal
System Maturity Matrix	[D-1-04]	Project Internal
Examples of products	[D-1-05]	Project Internal
Review Procedure Document	[D-1-06]	Project Internal
Review Data Package	[D-1-07]	Project Internal
Phase 1 Review Report Document	[D-1-08]	Project Internal
Detailed Processing Model Document	[D-2-01]	Public
Round Robin Assessment Report Document	[D-2-03]	Public
Data Production Status Report	[D-3-01]	Project Internal
Final Output Dataset	[D-3-01]	Public
Product Validation Plan	[D-4-01]	Project Internal
Product Validation Report : FDR	[D-4-02a]	Public
Product Validation Report : Sea-Ice TDP	[D-4-02b]	Public
Product Validation Report: Land-Ice TDP	[D-4-02c]	Public
Product Validation Report : Ocean Waves TDP	[D-4-02d]	Public
Product Validation Report : Ocean & Coastal TDP	[D-4-02e]	Public
Product Validation Report: Inland Waters TDP	[D-4-02f]	Public
Product Validation Report: Atmosphere TDP	[D-4-02g]	Public
Uncertainty Characterization Definition Document	[D-5-01]	Project Internal
Uncertainty Characterization Report	[D-5-02]	Public
Product User Guide	[D-5-03]	Public
Completeness Report ALT	[D-7-01]	Public
Completeness Report MWR	[D-7-02]	Public

Table 1 : List of FDR4ALT deliverables

Appendix B - Acronyms

AATSR	Advanced Along-Track Scanning Radiometer
AEM	Airborne electromagnetic
AIR	AIRWAVES2
AVISO	Archivage, Validation et Interprétation des données des Satellites Océanographiques
AMSR-E	Advanced Microwave Scanning Radiometer - Earth Observing System sensor
AMSU-A	Advanced Microwave Sounding Unit-A
ALT	Altimetry
ASSIST	Arctic Shipborne Sea Ice Standardization Too
ATM	Airborne Topographic Mapper
BDHI	Base de datos Hidrologica integrada
BGEP	Beaufort Gyre Exploration Project
CAL	Calibration
CCI	Climate Change Initiative
CFOSAT	Chinese-French Oceanic SATellite
CDS	Copernicus Data Service
CLS	Collecte Localisation Satellite
CMEMS	Copernicus Marine Environment Monitoring Service
CMSAF	Climate Monitoring Satellite Application Facility
CNES	Centre National des Etudes Spatiales
CRREL	Cold Regions Research and Engineering Laboratory
DAHITI	Database for Hydrological Time Series of Inland Waters
DGA	Direccion General de Aguas
ENVISAT	ENVIronment SATellite
EMD	Empirical mode decomposition
EO	Earth Observation
EPS	European Polar System
ERA	ECMWF Re-Analysis
ERS	European Remote-Sensing Satellite
ESA	European Space Agency
ESTEC	European Space Research and Technology Centre
FCDR	Fundamental Climate Data Record
FDR	Fundamental Data Records
FIDUCEO	Fidelity and uncertainty in climate data records from Earth Observations
FMR	Full Mission Reprocessing
FYI	First Year Ice
GEWEX	Global Energy and Water Exchanges
GFO	Geosat Follow-On
GIEMS	Global Inundation Extent from Multi-Satellites
GMSL	Global Mean Sea Level
GNSS	Global Navigation Satellite System
GPM	Global Precipitation Measurement
GRDC	Global Runoff Data Centre
G-REALM	Global Reservoir And Lake Monitor
G-VAP	GEWEX Water Vapour Assessment
HYBAM	HYdro-géochimie du Bassin AMazonien
ICARE	

IGM	Instituto Geografico Militar
IGN	Instituto Geografico Nacional
IMB	Ice Mass Balance
INA	Instituto Nacional de Agua
ISRO	Indian Space Research Organisation
IRPI	Istituto di Ricerca per la Protezione Idrogeologia
IWMI	International Water Management Institute
LEGOS	Laboratoire d'Etudes en Géophysique et Océanographie Spatiales
LIDAR	Ligth Detection And Ranging
LTAN	Local time of the ascending node
LWP	Liquid Water Path
MAC	Multisensor Advanced Climatology
MEAS-SIM	Measure-Simulation
MQE	Mean Quadratic Error
MSSH	Mean Sea Surface Height
MWR	Microwave Radiometer
NASA	National Aeronautics and Space Administration
NE	North East
NN	Neural Network
NPI	Norwegian Polar institute
NWP	Numerical Weather Prediction
NOAA	National Oceanic and Atmospheric Administration
OIB	Operation Ice Bridge
OLC	Open Loop Calibration
OSTST	Oceanography Surface Topography Science Team
POSTEL	Pôle d'Observation des Surfaces continentales par TELEdétection
PTR	Point Target Response
RD	Reference Document
REAPER	Reprocessing of Altimeter Products for ERS
RM	Review Meeting
RSS	Remote Sensing System
SALP	Service d'Altimétrie et de Localisation Précise
SARAL	Satellite with Argos and Altika
SLA	Sea Level Anomaly
SCICEX	Submarine Arctic Science Program
SGDR	Sensor Geophysical Data Record
SHOA	Servicio Hidrografico y Oceanografico de la Armada
SSB	Sea State Bias
SSH	Sea Surface Height
SSM/I	Special sensor microwave/imager
SST	Sea Surface Temperature
SWH	Significant Wave Height
SWIM	Surface Waves Investigation and Monitoring instrument
TAC	Thematic Assembly Center
TB	Température de Brillance (Brightness Temperature)
TDP	Thematic Data Products
TDS	Test Data Set
TFMRA	Threshold First-Maximum Retracker Algorithm
TMR	Topex Microwave Radiometer
TP	Topex/Poseidon

TCWV	Total column water vapour
VCC	Vicarious calibration
VS	Virtual Station
ULS	Upward Looking Sonar
USA	United States of America
USDA	United States Department of Agriculture
WHALES	Wave Height Adaptive Leading Edge Subwaveform
WTC	Wet Tropospheric Correction